NASA TECHNICAL NOTE

NASA TN D-2922

EFFECTS OF ASPECT RATIO AND CANOPY SHAPE ON LOW-SPEED AERODYNAMIC CHARACTERISTICS OF 50.0° SWEPT PARAWINGS

by Frank M. Bugg

Langley Research Center

Langley Station, Hampton, Va.

NATIONAL AERONAUTICS AND SPACE ADMINISTRATION • WASHINGTON, D. C. • JULY 1965

NASA TN D-2922

EFFECTS OF ASPECT RATIO AND CANOPY SHAPE ON LOW-SPEED AERODYNAMIC CHARACTERISTICS OF 50.0° SWEPT PARAWINGS

By Frank M. Bugg

Langley Research Center
Langley Station, Hampton, Va.

NATIONAL AERONAUTICS AND SPACE ADMINISTRATION

For sale by the Clearinghouse for Federal Scientific and Technical Information
Springfield, Virginia 22151 – Price $2.00

EFFECTS OF ASPECT RATIO AND CANOPY SHAPE ON LOW-SPEED AERODYNAMIC CHARACTERISTICS OF 50.0° SWEPT PARAWINGS

By Frank M. Bugg
Langley Research Center

SUMMARY

28638

An investigation was made to study the effects of aspect ratio and canopy shape on the static longitudinal and lateral aerodynamic characteristics of parawings having 50.0° sweptback leading edges. Parawings with conical canopies and aspect ratios of 3.00, 4.00, 5.00, and 5.45 and parawings with cylindrical (zero twist and camber) canopies and aspect ratios of 3.00, 4.00, and 5.45 were used in the investigation. Effects of canopy fullness were investigated for aspect-ratio-5.45 parawings with both conical and cylindrical canopies.

Maximum lift-drag ratios for the conical-canopy parawings varied from 5.2 to 5.9 as the aspect ratio increased from 3.00 to 5.45. Decreasing the canopy fullness of the aspect-ratio-5.45 conical-canopy parawing increased the maximum lift-drag ratio to 8.1. Increasing the aspect ratio of the cylindrical-canopy parawings from 3.00 to 5.45 increased the maximum lift-drag ratios from 7.3 to 11.8. The addition of a small amount of twist and camber to the aspect-ratio-5.45 cylindrical canopy parawing by increasing the canopy fullness increased the maximum lift-drag ratio to 16.9 and improved the lift-drag ratios at high lift.

Parawings with conical canopies had extrapolated pitching-moment coefficients at zero lift that were negative at low aspect ratio and became less negative as the aspect ratio increased until at an aspect ratio of 5.45 a positive value was indicated. For the cylindrical-canopy parawings, the pitching-moment coefficient at zero lift was negative and became more negative with increasing aspect ratio for all configurations investigated.

A comparison of experimental longitudinal aerodynamic characteristics with estimates based on wing theory showed fairly good agreement for parawings having the least amount of canopy curvature. Estimated results, particularly pitching-moment characteristics, did not agree well with experimental results for parawings having large amounts of canopy curvature.

INTRODUCTION

The National Aeronautics and Space Administration has conducted a number of research investigations to determine the aerodynamic characteristics of parawings. (For example, see refs. 1 to 3.) Much of the research to date has been concerned with studies of parawings as recovery devices for space vehicles and rocket boosters for which low-to-medium glide capabilities were required. The parawing which received the most attention in studies of these applications was of low aspect ratio and had a highly twisted and cambered conical canopy with equal-length leading edges and keel. Results of general research investigations on this parawing are given in reference 2 for a wide range of sweep angles and canopy fullness and in reference 3 for a parawing having large-diameter leading edges simulating an inflated-tube structure. The low-aspect-ratio conical parawing may be adequate for applications in which only a moderate glide range is required. For other applications, such as tow vehicles or where extended glide range is needed, a wing with a higher lift-drag ratio would be desirable. Initial work on high-performance parawings reported in reference 1 indicated that significant increases in maximum lift-drag ratio could be obtained from higher-aspect-ratio conical wings and wings with cylindrical canopies which provided essentially zero camber and twist and still maintained the tension-lifting-surface concept.

The purpose of the present investigation was to extend the experimental and theoretical work of reference 1 to include a systematic variation of aspect ratio and canopy fullness for both conical and cylindrical wings. Effects of aspect ratio were studied on 50.0° swept wings having conical and cylindrical canopies for a range of aspect ratios from 3.00 to 5.45. The effects of canopy fullness were investigated for an aspect ratio of 5.45 for both the conical and cylindrical canopies. All models had small rigid leading edges and keel; a spreader bar was used to maintain the fixed leading-edge sweep of 50.0°. Longitudinal aerodynamic characteristics were obtained at 0° sideslip through an angle-of-attack range that extended from the onset of canopy luffing at low lift coefficients to angles of attack beyond the stall. Lateral stability derivatives were obtained over approximately the same angle-of-attack range at sideslip angles of ±4° for most of the wings investigated.

SYMBOLS

The force and moment coefficients are presented with respect to the body system of axes except for lift and drag coefficients which are presented with respect to the wind axes. The positive directions of forces and moments are shown in figure 1. The moments are given about a reference point on the keel center line positioned longitudinally at the 25-percent-chord point of the mean aerodynamic chord. Reference areas and lengths used in the reduction of data are presented in table I and are based on the projected 50.0° swept-wing planform, with the trailing edge taken as a straight line connecting the wing tip and the trailing edge of the root chord.

A	aspect ratio
b	parawing span, in.
c	local parawing chord, measured parallel to keel, in.
c_{av}	average parawing chord, in.
$\bar{c}$	parawing mean aerodynamic chord, in.
C_A	axial-force coefficient, $\frac{\text{Axial force}}{qS}$
C_D	drag coefficient, $\frac{\text{Drag}}{qS}$
c_l	section lift coefficient, $\frac{\text{Section lift}}{qc}$
C_L	lift coefficient, $\frac{\text{Lift}}{qS}$
C_l	rolling-moment coefficient, $\frac{\text{Rolling moment}}{qSb}$
$C_{L,max}$	maximum lift coefficient
C_{L_α}	lift-curve slope per degree
C_{l_β}	effective-dihedral parameter, $\frac{\Delta C_l}{\Delta\beta}$, per deg
C_m	pitching-moment coefficient, $\frac{\text{Pitching moment}}{qS\bar{c}}$
$C_{m,o}$	extrapolated pitching-moment coefficient at $C_L = 0$
$\frac{\partial C_m}{\partial C_L}$	static-longitudinal-stability parameter
C_n	yawing-moment coefficient, $\frac{\text{Yawing moment}}{qSb}$
C_N	normal-force coefficient, $\frac{\text{Normal force}}{qS}$
C_{n_β}	directional-stability parameter, $\frac{\Delta C_n}{\Delta\beta}$, per deg

C_Y side-force coefficient, $\frac{\text{Side force}}{qS}$

C_{Y_β} side-force parameter, $\frac{\Delta C_Y}{\Delta \beta}$, per deg

L/D lift-drag ratio

$(L/D)_{max}$ maximum lift-drag ratio

q free-stream dynamic pressure, lb/sq ft

S projected area of wing, sq ft (see table I)

x_{cp} distance from leading edge of mean aerodynamic chord to center of pressure, measured parallel to keel in fraction of $\bar{c}$, in.

y spanwise distance from plane of symmetry, ft

α angle of attack of parawing keel, deg

α_o angle of attack of parawing keel at zero lift, deg

β sideslip angle, deg

ϵ geometric twist angle between a line connecting leading edge and trailing edge of a section and reference plane containing parawing keel and wing tips, positive for washout, deg

Λ_o sweepback of leading edge of canopy flat pattern, deg

MODEL DESCRIPTION

The parawing models had metal frames to which fabric canopies were attached. Sketches of the models and canopy flat patterns are presented in figures 2 to 4 for the conical and cylindrical canopies. The surfaces of the conical-canopy parawings were assumed to lie on two right circular cones which intersected at the wing apex as illustrated in the following sketch:

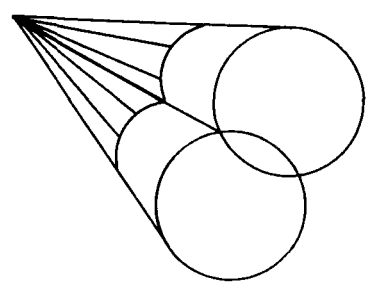

constructed so that the warp of the fabric was parallel to the canopy trailing edge. The geometric characteristics of the canopy flat patterns and the fabric material used for each canopy are given in table II.

TESTS

All tests were conducted at atmospheric stagnation pressure in the Langley high-speed 7- by 10-foot tunnel at dynamic pressures of 6 and 8 lb/sq ft. Because the leading edges of the conical wings deflected appreciably at the highest test dynamic pressure, data for these wings are presented only for $q = 6$ lb/sq ft. For greater accuracy, however, data are desired at the highest possible dynamic pressure, and inasmuch as the leading edges on the cylindrical wings were much less flexible than those on the conical wings, results for the cylindrical wings are presented for $q = 8$ lb/sq ft. All data presented were obtained with transition free. Reynolds numbers based on the length of the reference mean aerodynamic chord are given in the following table:

Parawing canopy	q, lb/sq ft	Reynolds number for -			
		A = 3.00	A = 4.00	A = 5.00	A = 5.45
Conical	6	963,000	722,000	578,000	529,000
Cylindrical	8	1,142,000	856,000		628,000

Static longitudinal aerodynamic characteristics were obtained at 0° sideslip through an angle-of-attack range from the canopy luffing condition at low angles to angles beyond the stall. The variable-angle sting support was limited to a 24° angle-of-attack range, but by the use of appropriate couplings on the sting, each model was tested through overlapping angle-of-attack ranges in order to achieve the desired angles of attack. Static lateral stability characteristics were obtained through approximately the same angle-of-attack range and at $\pm 4^\circ$ sideslip for all wings except the aspect-ratio-5.00 conical wing and the aspect-ratio-5.45 and $\Lambda_o = 48.2^\circ$ cylindrical wing for which measurements were made at $\pm 5^\circ$ sideslip.

CORRECTIONS

For most of the data, no jet-boundary or blockage corrections were applied because these corrections have been found to be negligible for the size of models tested with the tunnel-wall perforated slots open. The aspect-ratio-5.00 conical wing and the aspect-ratio-5.45 and $\Lambda_o = 48.2^\circ$ cylindrical wing were tested during a period when the test-section slots were closed and these data were therefore corrected for jet-boundary and blockage effects by the methods of references 4 and 5. Corrections were also applied to the angles of

attack and sideslip to account for effects of deflections of the sting and balance under aerodynamic load.

The aerodynamic characteristics presented in reference 1 were corrected for effects of the spreader bar and balance housing and the application of corresponding corrections to the present data was considered desirable. Inasmuch as a different spreader-bar arrangement was used in the present tests, a new set of tare corrections were obtained. The tares of the spreader bar and balance housing were originally measured in the free stream with the wing removed. When these tare corrections were applied to the present data, the resulting maximum lift-drag ratio for the high-aspect-ratio cylindrical wing was unreasonably high and above the estimated value for an ideal wing of the same aspect ratio. Inasmuch as the spreader bar in the present investigation was relatively close to the wing surface, especially for the cylindrical wings (fig. 3), the effects of the wing flow field on the spreader bar were studied. Accordingly, aerodynamic characteristics of the spreader bar used on the cylindrical wings and of the balance housing were measured with these components in the presence of, but not attached to, the cylindrical wings for an angle-of-attack range from -2° to 45°. The wing support used in the determination of these tares is shown in figure 6. This apparatus replaced the spreader bar and keel of the parawing and attached the parawing rigidly to the sting. The measured tare corrections applied to the data are presented in figure 7. The lift and drag tare corrections presented were subtracted from the data and, in addition, a pitching-moment tare correction of 0.003 was subtracted from the data for the $A = 5.45$ wings. The pitching-moment tare was negligible for the wings of low aspect ratio and therefore no correction was applied. Figure 8 gives conical-wing lift-drag ratios before and after spreader-bar and balance-housing tare corrections.

PRESENTATION OF RESULTS

Results of the present parawing investigation are presented in figures 9 to 19. An outline of the contents of the data figures is as follows:

RESULTS AND DISCUSSION

The extreme variations in wing geometric characteristics, primarily in twist and camber, encountered in this investigation would be expected to cause corresponding large differences in certain aerodynamic characteristics. Methods for estimating some of the important longitudinal aerodynamic characteristics by means of wing theory are given in reference 1 and it was considered desirable to determine how well these estimates could predict the effects of the large variations in planform and wing shape encountered in the present study. In order to compare experimental values with the estimates, the analysis of test results is made in terms of the following parameters: zero-lift angle of attack α_o, pitching-moment coefficient at zero lift $C_{m,o}$, lift-curve slope C_{L_α}, static-longitudinal-stability parameter $\frac{\partial C_m}{\partial C_L}$, maximum lift-drag ratio $(L/D)_{max}$, and maximum lift coefficient $C_{L,max}$.

The test results did not extend to zero lift because of canopy luffing at low lift and, therefore, the parameters α_o and $C_{m,o}$ were obtained by extrapolation of the data to zero lift. The pitching-moment curves were generally nonlinear and therefore the experimental values of $\frac{\partial C_m}{\partial C_L}$ and $C_{m,o}$ are representative of only a small portion of each curve; however, these data provide some indication of the influence of aspect ratio and canopy shape. The estimated and experimental longitudinal parameters are compared after discussion of the test results.

Effect of Aspect Ratio on Longitudinal Aerodynamic Characteristics

Lift characteristics.- Increasing the aspect ratio on both the conical (fig. 9) and the cylindrical parawings (fig. 13) increased the lift-curve slope and increased the maximum lift coefficient (fig. 17). The zero-lift angle of attack was positive and increased slightly for the conical wings, whereas it was slightly negative for the cylindrical wings and became more negative as the aspect ratio increased. (See fig. 17.)

Maximum lift-drag ratios.- Maximum lift-drag ratios of the conical wings with 45.0° flat-pattern sweep showed a small increase from about 5.2 to 5.9 as the aspect ratio increased from 3.00 to 5.45 (fig. 17). The cylindrical wings with 48.2° flat-pattern sweep, on the other hand, showed an increase from about 7.3 to 11.8 as the aspect ratio varied from 3.00 to 5.45. Both the overall level of $(L/D)_{max}$ and the increase with aspect ratio for the conical wings appear low on the basis of the results presented in reference 1. The main difference in the lift-drag ratios is believed to arise from differences in the magnitude of the tare drag attributed to the spreader bar and the balance housing between this investigation and reference 1. In the present investigation the effects of the cylindrical-wing flow field on the spreader-bar and

balance-housing drag were accounted for; whereas in the investigation of reference 1, the tare measurements were made with the spreader bar and balance housing in the free stream. However, the effects of the spreader-bar flow field on the wing canopy were not determined in either investigation. Because the cylindrical canopy was much closer to the spreader bar than was the conical canopy and because the cylindrical-wing tares were used to correct the results for both wings, the tares measured in the cylindrical-wing flow field probably gave conservative values of lift-drag ratio when applied to the conical-wing data of the present investigation. A comparison between lift-drag ratios of reference 1 and the present investigation for conical wings with and without spreader-bar and balance-housing tare corrections is given in figure 8 and shows that relatively small differences in lift-drag ratios existed before application of the tare drag.

Pitching-moment characteristics.- The extrapolated pitching-moment coefficient at zero lift was negative for an aspect ratio of 3.00 for both the conical and cylindrical parawings (fig. 17). For the conical wings increasing the aspect ratio caused the pitching-moment coefficient at zero lift to become less negative until at an aspect ratio of 5.45 a positive value of $C_{m,o}$ was indicated. For the cylindrical wings, on the other hand, increasing negative values of $C_{m,o}$ were observed as the aspect ratio increased. The values of $C_{m,o}$ presented in figure 17, as previously mentioned, apply for only a restricted lift range; however, the trends showing effects of aspect ratio in this figure do provide a good overall indication of the shifts in the pitching-moment curves presented in figures 9 and 13. The same observation can be made with regard to $\frac{\partial C_m}{\partial C_L}$ in that the overall level of stability was somewhat less for an aspect ratio of 5.45 than for an aspect ratio of 3.00. All the wings showed a stable break in pitching moments following wing stall; however, there appeared to be somewhat greater instability preceding stall for the high-aspect-ratio cylindrical wings than for the conical wings.

A possible longitudinal stability problem, not directly indicated in the pitching-moment data of figure 9, has been encountered in wind-tunnel and flight tests of parawing vehicles that exhibit an abrupt stall above maximum lift. This problem, which is characterized by a deep-stall pitch-up, can arise for a parawing vehicle having a center of gravity located well below the wing if there is a large loss in the normally high negative value of axial force accompanying wing stall. Some of the conical and cylindrical wings investigated showed losses in axial force at high angles of attack and an assessment of the usefulness of a particular wing should include an examination of the longitudinal stability at angles of attack above the stall.

Effect of Canopy Fullness on Longitudinal Aerodynamic Characteristics

Large changes in all the longitudinal parameters accompanied variations in canopy fullness because of the extreme changes in wing camber and twist that occurred as the flat-pattern sweep varied for the conical parawings. (See

Streamwise airfoil contours as defined by the surface of the cones were computed by the method given in reference 1 and some of the calculated twist and camber results for the $A = 5.45$ conical parawings are given in figure 5.

The surfaces of the cylindrical-canopy parawings were assumed to lie on two cylinders which had their axes parallel to the keel as shown in the following sketch:

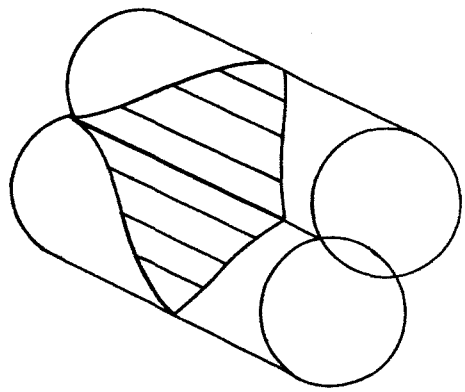

Inasmuch as all the streamwise sections were assumed to be parallel to the keel, the basic cylindrical wings $(\Lambda_o = 48.2^o)$ were assumed to have no twist or camber.

Aspect ratios of 3.00, 4.00, 5.00, and 5.45 for the conical wings and aspect ratios of 3.00, 4.00, and 5.45 for the cylindrical wings were obtained by changing the canopy root chord while retaining the same leading edges and spreader bar. The leading edges used on both types of wings in this investigation are the same as those employed in the investigation reported in reference 1.

The canopies for the conical wings were constructed with the sweep of the leading edge of the flat pattern less than the 50.0^o sweep angle of the frame. The canopy fullness (and the resulting camber and twist) was varied for the aspect-ratio-5.45 conical wings by using canopies with flat-pattern sweep angles of 35.0^o, 40.0^o, 42.5^o, 45.0^o, and 47.5^o. (See fig. 4.)

The leading edges of the cylindrical wings had a helical shape inasmuch as they were formed about cylinders and the average sweep angle was 50.0^o. (See fig. 3.) A canopy flat-pattern sweep angle of 48.2^o provided a parawing on the assumed cylinders with a zero twist and camber and 50.0^o leading-edge sweep. The fullness of the aspect-ratio-5.45 cylindrical canopies was increased by the use of flat-pattern sweep angles of 44.0^o and 46.0^o. (See fig. 4.) Although these models are referred to as cylindrical-canopy parawings, only the leading edges were designed to conform to the assumed cylindrical shape.

The canopies for all the parawings were attached to the top of the keel and to the leading edges as shown in figures 2 and 3. The canopies were

fig. 5.) The computed values of camber and twist for the conical wings may not represent the actual shape of the flexible wing canopy throughout the angle-of-attack range; however, they do provide a very good indication of the changes in wing shape with flat-pattern sweep.

Computed values of twist and camber for the $\Lambda_o = 44.0$ and 46.0° cylindrical wings are not presented because of difficulties encountered in defining their shapes. Some estimates were made, however, by use of the assumption that the trailing edge was a circular arc having a length equal to the canopy flat-pattern trailing-edge length. These estimates indicated that the twist was very low for the cylindrical wings in comparison with the twist for the conical wings. One of the problems encountered in defining the twist of the cylindrical wings was that the basic $(\Lambda_o = 48.2^\circ)$ zero-twist cylindrical wing appeared, from the observed angle of attack and pitching moment at zero lift, to have washin. Inasmuch as the angle of attack for zero lift has been found to provide a good indication of the overall effective twist for conical parawings, it is used in subsequent sections to relate the test results obtained for the cylindrical and conical wings.

Lift characteristics.- The angle of attack for zero lift for the conical parawings decreased from a value of about 18° to 7.5° (fig. 18) as the flat-pattern sweep increased from 35.0° to 47.5° (decreasing canopy fullness). The value of α_o for the cylindrical parawings decreased from about 3° to -3° as the flat-pattern sweep increased from 44.0° to 48.2° (fig. 18). The negative value obtained for $\Lambda_o = 48.2^\circ$ indicates that the wing had washin, as mentioned previously, and observations made during the tests also showed that the canopy lobe was distorted from a cylindrical shape. The distortion observed was such that the inboard portion of the trailing edge was higher than the leading edge and the outboard portion was below the top of the leading edge. It is therefore believed that distortion of the canopy from the cylindrical shape under air load caused the negative value at zero lift of both the angle of attack and the pitching moment of the cylindrical wings.

The maximum lift coefficients of the conical parawings increased as the flat-pattern sweep increased from 35.0° to 42.5°; further decreases in canopy fullness caused a reduction in maximum lift. (See fig. 18.) For the cylindrical parawings $(\Lambda_o = 44.0^\circ$, 46.0°, and $48.2^\circ)$, the maximum lift coefficient also decreased as the canopy fullness was decreased. The beneficial effect of some canopy fullness (small amount of washout) on maximum lift coefficient is consistent with experience on conventional wings for which improvement in $C_{L,max}$ can be effected by adding some washout near the tip. Apparently the variation of twist across the span of the $\Lambda_o = 35.0^\circ$ and $\Lambda_o = 40.0^\circ$ conical wings was so extreme that local stalling may have existed somewhere on the wings throughout the test angle-of-attack range.

Maximum lift-drag ratios.- Values of maximum lift-drag ratio for the $A = 5.45$ conical parawings increased from 3.2 to 8.1 as the flat-pattern sweep increased from 35.0° to 47.5° (fig. 18). Maximum lift-drag ratios for the $A = 5.45$ cylindrical wings increased from 11.2 to 16.9 as the flat-pattern sweep increased from 44.0° to 46.0°. Increasing the flat-pattern sweep to 48.2° caused the maximum lift-drag ratio to decrease to a value of 11.8 and also

caused a decrease in lift-drag ratio at high lift (fig. 15). Maximum lift-drag ratios for the cylindrical wings were generally about twice the values obtained for the conical wings at the same flat-pattern sweep (fig. 18). Since the lift-drag ratios were greatly dependent on wing twist and the twist of the two types of wings were probably much different at a given flat-pattern sweep, the results presented in figure 19 may afford a more meaningful comparison than those given in figure 18. If the wing zero-lift angle is interpreted as indicating effective wing twist, then it appears from the results of figure 19 that the highest maximum lift-drag ratio occurred for the wing having a small amount of washout and that the performance characteristics of the cylindrical and conical wings are directly related through the effective wing twist.

Pitching-moment characteristics.- Large effects of canopy fullness on pitching moments were indicated for the conical parawings, and the overall effects are summarized in figures 18 and 19. These results and the basic data of figure 11 show that increasing the flat-pattern sweep (decreasing canopy fullness) from 35.0° to 45.0° provided positive increments in $C_{m,o}$ and increased the longitudinal stability at moderate lift. For the cylindrical parawings, decreasing the canopy fullness from $\Lambda_o = 44.0^\circ$ to $\Lambda_o = 48.2^\circ$ caused the value of $C_{m,o}$ to become more negative and the longitudinal stability to decrease. The pitching-moment characteristics presented in figure 19 for the conical and cylindrical wings appear, as had the lift-drag ratios, to be related to the amount of effective wing twist. Negative values of $C_{m,o}$ occurred for the $A = 5.45$ cylindrical wings having a small amount of twist, and positive values of $C_{m,o}$ occurred for all but the higher twist conical wings. The occurrence of negative $C_{m,o}$ at high twist $(\Lambda_o = 35.0^\circ)$ may have been caused by negative stall of sections near the tips where the washout was very high (fig. 5).

Longitudinal stability $\frac{\partial C_m}{\partial C_L}$ (fig. 19) was the highest for wings having a small amount of washout and decreased rapidly as the effective twist became greater. The variation of pitching-moment coefficient with lift coefficient showed that a pitch-up tendency occurred before stall with the smallest amount of canopy fullness for both the conical and cylindrical wings (figs. 11 and 15). This occurrence of longitudinal instability was greatly alleviated by increasing the canopy fullness.

Effect of Aspect Ratio on Lateral Stability Characteristics

The static lateral stability derivatives are presented about a reference point on the center line of the parawing keel at the quarter-chord point of the mean aerodynamic chord. To represent a particular parawing application these data should be transferred to the desired reference point for the complete vehicle; this reference point is generally below the parawing keel.

For the conical parawings with $\Lambda_o = 45.0^\circ$, the value of the directional-stability parameter C_{n_β} was generally positive up to the approach of wing stall after which directional instability was indicated (fig. 10). Increasing

the aspect ratio from 3.00 to 5.45 for these wings increased the positive value of C_{n_β} in the operational angle-of-attack range. There seemed to be no consistent effect of aspect ratio on the value of the effective-dihedral parameter, but at angles of attack above about 39° there was a general decrease in the effective-dihedral parameter $\left(-C_{l_\beta}\right)$ and at lower angles of attack the aspect-ratio-5.45 wing had the lowest effective dihedral.

All the cylindrical parawings generally had low values of C_{n_β} and some directional instability in the operational angle-of-attack range. (See figs. 14 and 16.) These wings generally had large negative values of C_{l_β} below the stall. For both the directional-stability parameter and the effective-dihedral parameter there appeared to be no consistent effect of changes in either aspect ratio or flat-pattern sweep.

Effect of Canopy Fullness on Lateral Stability Characteristics

The directional-stability parameter C_{n_β} increased with increasing flat-pattern sweep for the aspect-ratio-5.45 conical wings at angles of attack below 25°. (See fig. 12.) At wing stall the wings with least canopy fullness $\left(\Lambda_o = 45.0^\circ \text{ and } \Lambda_o = 47.5^\circ\right)$ showed some directional instability. Below the wing stall there was a general decrease of effective dihedral with decreased canopy fullness, except for the change in fullness from $\Lambda_o = 45.0^\circ$ to $\Lambda_o = 47.5^\circ$ during which a large increase in effective dihedral occurred.

Comparison of Experimental and Estimated Longitudinal Aerodynamic Characteristics

Angle of attack for zero lift.- Theoretical and experimental effects of aspect ratio and canopy fullness are presented in figures 17 and 18; the theoretical results were obtained from data based on the wing theory of reference 1. For the conical parawings, the estimated variations of zero-lift angle of attack with aspect ratio (fig. 17) and flat-pattern sweep (fig. 18) are in good agreement with the experimental results. Experimental values were somewhat lower than estimated values and this type of agreement is consistent with most parawing configurations investigated. (For example, see ref. 1.) In view of the extreme variations in camber and twist for the wings investigated, it is believed that the estimates provide a good indication of the effects of aspect ratio and canopy fullness on the zero-lift angle of attack for conical parawings. The use of an empirical correction of -3° or -4° added to the estimated angle should afford an excellent estimate of the zero-lift angle for a wide variety of conical parawings.

The estimated zero-lift angle of attack for a zero-twist cylindrical parawing would, of course, be 0°. The results of figure 17 indicate good agreement

between theory and experiment at $A = 3.00$ for the cylindrical wings; however, at $A = 5.45$ experimental results gave a value of about -3°. Estimates were not made for the effects of canopy fullness on cylindrical wings because of the aforementioned difficulties encountered in defining a shape for calculation of twist angles. It is believed, therefore, that the experimental results presented herein and in reference 1 could be used as the most reliable indication of the zero-lift angle for cylindrical parawings until further information is available.

Lift-curve slopes.- Estimates of lift-curve slopes were obtained from the wing theory of reference 1, in which a section lift slope of 0.09 per degree was assumed. The estimated results were for planar wings and therefore varied only with aspect ratio; no modifications have been made to account for curvature of the lifting surface (canopy fullness). Comparison between estimated and experimental lift-curve slopes (fig. 17) shows that the estimates are somewhat high in relation to data for the conical wings below $A = 5$. The estimated increase in C_{L_α} with aspect ratio from $A = 3.00$ to 5.45 was considerably less than the experimental increase over the same range of aspect ratios for both the conical and cylindrical wings. Experimental effects of canopy fullness on the conical wings (fig. 18) indicate that a good estimate of C_{L_α} would be expected only for canopies having very shallow lobes $(\Lambda_o = 45.0^{\circ})$.

The large difference between experimental and estimated values of C_{L_α} for large amounts of canopy fullness may have occurred as a result of one factor or a combination of several factors. For example, at low and moderate lift coefficients where canopy distortion and some trailing-edge flutter occur for deep-lobe canopies, nonpotential flow conditions probably exist over a large part of the wing. Another important consideration is the use of planar wing theory to estimate the characteristics of a highly nonplanar, curved lifting surface. It is believed, therefore, that conventional wing theory may provide a fairly good estimate of C_{L_α} for parawings having very shallow lobes, but cannot be used with assurance for parawings having deep canopy lobes.

Maximum lift-drag ratios.- No attempt has been made to estimate the maximum lift-drag ratios for the wings in the present investigation; however, an ideal upper bound has been approximated as an aid in determining to what extent each wing attained the performance potential available. In determining the ideal variation, the skin-friction drag of each of the canopies was estimated and used with the assumption that the drag due to lift was $\frac{C_L^2}{\pi A}$. Inasmuch as the leading edges of the models were small, most of the difference between the experimental and the ideal curves can be attributed to the effects of twist and camber on minimum drag and drag due to lift.

Experimental results showing effects of aspect ratio (fig. 17) indicate very little change in $(L/D)_{max}$ for the conical wings, whereas results for the cylindrical wings show an increase in $(L/D)_{max}$ of the same magnitude as that of the ideal variation. The level of maximum lift-drag ratios indicates that the conical wings were capable of realizing only about 30 percent of the ideal maximum lift-drag ratios, whereas the cylindrical wings gave 46 to 57 percent

of the ideal. Increasing the canopy fullness (fig. 18) of the cylindrical wing from $\Lambda_o = 48.2^o$ to $\Lambda_o = 46.0^o$ allowed 85 percent of the ideal maximum lift-drag ratio to be obtained. A further increase in canopy fullness, however, gradually decreased $(L/D)_{max}$ to a lesser percent of the ideal than the percentage obtained at $\Lambda_o = 48.2^o$.

The large differences in lift-drag ratios obtained for the conical and cylindrical wings are believed to arise from the drag associated with the basic span loading due to twist for the conical wings (ref. 1). The following sketches illustrate the type of span loading on the cylindrical and conical wings at a lift coefficient near the ideal C_L for $(L/D)_{max}$:

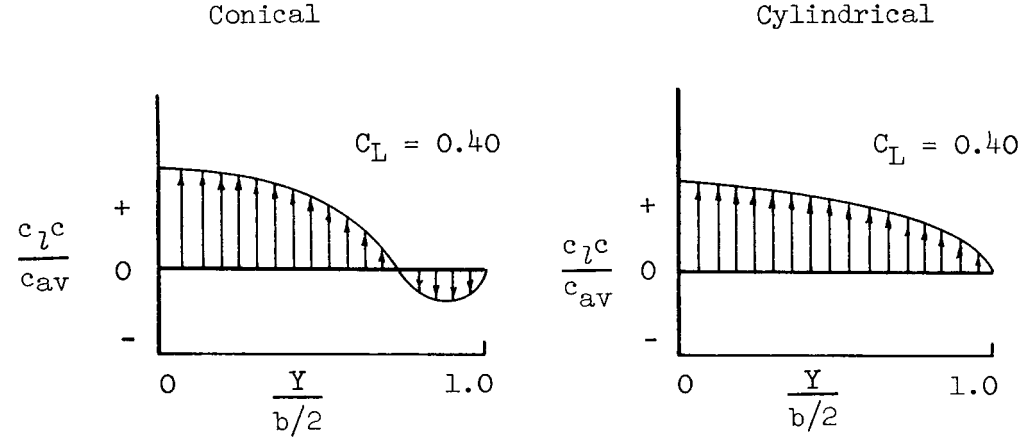

The large washout near the tip of the conical wing can produce a span loading with a negative load carried near the tip as shown in the sketch. This type of span loading would be expected to produce relatively high induced drag in comparison with the drag produced by the more nearly elliptical load distribution shown for the cylindrical wing.

Pitching-moment characteristics.- The comparison between estimated and experimental pitching-moment characteristics presented in reference 1 was fairly good and suggested that these characteristics for parawings might be predicted from conventional wing theory with reasonable accuracy. Generally the present results substantiate this correlation; however, the extended range of variables covered in the present study has revealed some significant discrepancies between estimates and experimental results. For example, the variation with aspect ratio of estimated and experimental $C_{m,o}$ agreed well for the conical wings (fig. 17), whereas the variation of estimated $C_{m,o}$ with canopy fullness decreased while the variation of experimental $C_{m,o}$ with canopy fullness increased (fig. 18). Estimates of the effects of both aspect ratio and canopy fullness on longitudinal stability for conical wings (figs. 17 and 18) were generally so different from experimental results that the few points of agreement shown may have been fortuitous. As might have been expected, the agreement between experimental and estimated values of $C_{m,o}$ and $\frac{\partial C_m}{\partial C_L}$ appeared to be somewhat better for the wing canopies having the smallest twist (fig. 18). These results indicate, therefore, that conventional planar wing theory as

applied in the present estimates cannot be used to predict reliably the pitching-moment characteristics of conical parawings having appreciable canopy fullness. The sources of the discrepancies have not yet been determined; however, some possibilities are readily apparent. The use of planar wing theory for a wing having a highly curved lifting surface, for example, neglects the effect of vertical displacement of the center of pressure on $C_{m,o}$. Another possible source of discrepancy is the fact that the shape of the flexible lifting surface probably did not conform to the true conical shape that was assumed for the estimates.

The fairly good agreement noted for the estimated and experimental zero-lift angles and the poor agreement of pitching-moment characteristics suggest that the overall load can be estimated with much greater reliability than can the effects of the load distribution. It is therefore believed that refinements in the estimation of span-load distribution will have to be made before reliable estimates of the pitching-moment characteristics can be obtained. Until more reliable procedures are developed, existing experimental data should be used as a basis for empirical estimates of the pitching-moment characteristics of parawings.

CONCLUSIONS

An investigation of a series of parawings having conical and cylindrical canopies indicated the following conclusions:

1. Maximum lift-drag ratios for the conical parawings with 45.0° flat-pattern sweep varied from 5.2 to 5.9 as the aspect ratio was increased from 3.00 to 5.45. Decreasing the canopy fullness of the aspect-ratio-5.45 conical wing by increasing the flat-pattern sweep to 47.5° increased the maximum lift-drag ratio to 8.1.

2. Increasing the aspect ratio from 3.00 to 5.45 for the 48.2° flat-pattern sweep cylindrical parawings increased the maximum lift-drag ratios from 7.3 to 11.8. The addition of a small amount of twist and camber to the aspect-ratio-5.45 cylindrical wing by increasing the canopy fullness increased the maximum lift-drag ratio to 16.9 and improved the lift-drag ratios at high lift.

3. Parawings with conical canopies had extrapolated pitching-moment coefficients at zero lift that were negative at low aspect ratio and became less negative as the aspect ratio increased until at an aspect ratio of 5.45 a positive value was indicated. For parawings with cylindrical canopies, the pitching-moment coefficients at zero lift were negative and became more negative with increasing aspect ratio for all configurations investigated.

4. A comparison of experimental longitudinal aerodynamic characteristics with estimates based on conventional wing theory showed fairly good agreement for parawings having the least amount of canopy curvature. Estimated results, particularly pitching-moment characteristics, did not agree well with experimental results for parawings having large amounts of canopy curvature.

5. Lateral stability derivatives obtained for the conical parawings indicated positive static directional stability for angles of attack up to the approach of wing stall. Near the stall a loss in directional stability and effective dihedral occurred.

6. The cylindrical-canopy parawings exhibited generally poor static directional stability throughout the angle-of-attack range. Fairly large positive values of effective-dihedral parameter were indicated for the cylindrical-canopy wings at high angles of attack.

Langley Research Center,
National Aeronautics and Space Administration,
Langley Station, Hampton, Va., May 6, 1965.

REFERENCES

1. Polhamus, Edward C.; and Naeseth, Rodger L.: Experimental and Theoretical Studies of the Effects of Camber and Twist on the Aerodynamic Characteristics of Parawings Having Nominal Aspect Ratios of 3 and 6. NASA TN D-972, 1963.

2. Naeseth, Rodger L.; and Gainer, Thomas G.: Low-Speed Investigation of the Effects of Wing Sweep on the Aerodynamic Characteristics of Parawings Having Equal-Length Leading Edges and Keel. NASA TN D-1957, 1963.

3. Croom, Delwin R.; Naeseth, Rodger L.; and Sleeman, William C., Jr.: Effects of Canopy Shape on Low-Speed Aerodynamic Characteristics of a 55° Swept Parawing With Large-Diameter Leading Edges. NASA TN D-2551, 1964.

4. Gillis, Clarence L.; Polhamus, Edward C.; and Gray, Joseph L., Jr.: Charts for Determining Jet-Boundary Corrections for Complete Models in 7- by 10-Foot Closed Rectangular Wind Tunnels. NACA WR L-123, 1945. (Formerly NACA ARR L5G31.)

5. Herriot, John G.: Blockage Corrections for Three-Dimensional-Flow Closed-Throat Wind Tunnels, With Consideration of the Effect of Compressibility. NACA Rept. 995, 1950. (Supersedes NACA RM A7B28.)

TABLE I.- PROJECTED-PLANFORM CHARACTERISTICS

Parawing canopy	Aspect ratio	Sweep, deg	Root chord, in.	$\bar{c}$, in.	b, in.	S, sq ft
Conical	3.00	50	42.80	28.55	64.28	9.55
	4.00	↓	32.14	21.44	↓	7.17
	5.00	↓	25.71	17.14	↓	5.74
	5.45	↓	23.57	15.71	↓	5.26
Cylindrical	3.00	[a]50	42.80	28.55	64.28	9.55
	4.00	↓	32.14	21.44	↓	7.17
	5.45	↓	23.57	15.71	↓	5.26

[a]Average value.

TABLE II.- CANOPY-FLAT-PATTERN CHARACTERISTICS

Parawing canopy	Aspect ratio	Sweep, deg	Span, in.	Area, sq ft	Fabric
Conical	3.30	45.0	70.71	10.51	Dacron
	4.40	45.0	↓	7.89	↓
	5.50	45.0	↓	6.31	↓
	5.73	47.5	67.56	5.33	Acrylic-coated rip-stop nylon
	6.00	45.0	70.71	5.79	Nylon-Mylar
	6.26	42.5	73.73	6.03	Acrylic-coated rip-stop nylon
	6.50	40.0	76.60	6.27	↓
	6.95	35.0	81.92	6.70	↓
Cylindrical	3.20	48.2	68.44	10.17	Nylon-Mylar
	4.26	48.2	↓	7.64	↓
	5.81	48.2	↓	5.60	Dacron
	6.06	46.0	71.37	5.84	Nylon-Mylar
	6.27	44.0	73.90	6.05	↓

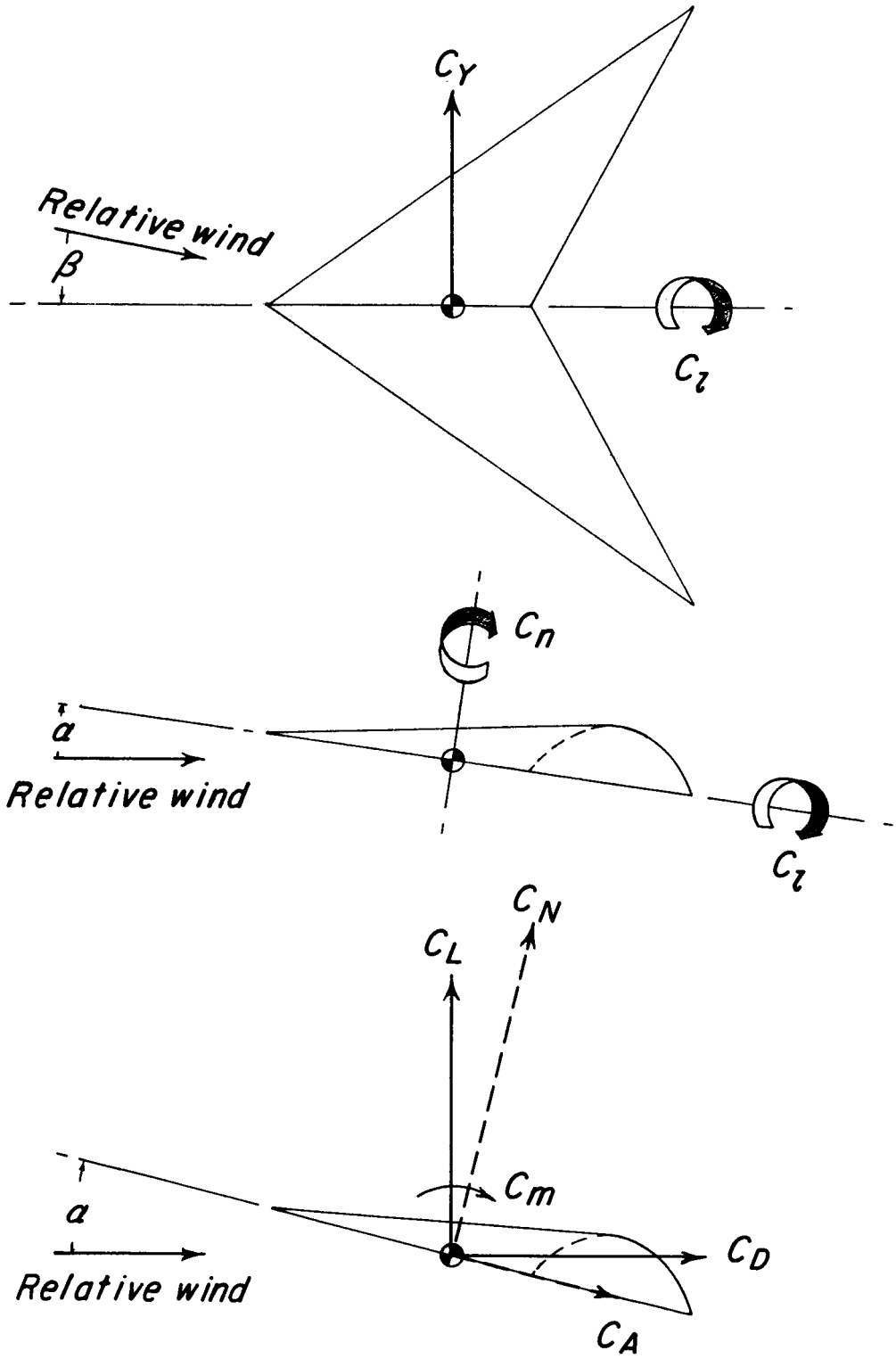

Figure 1.- Systems of axes and convention used to define positive sense of forces, moments, and angles.

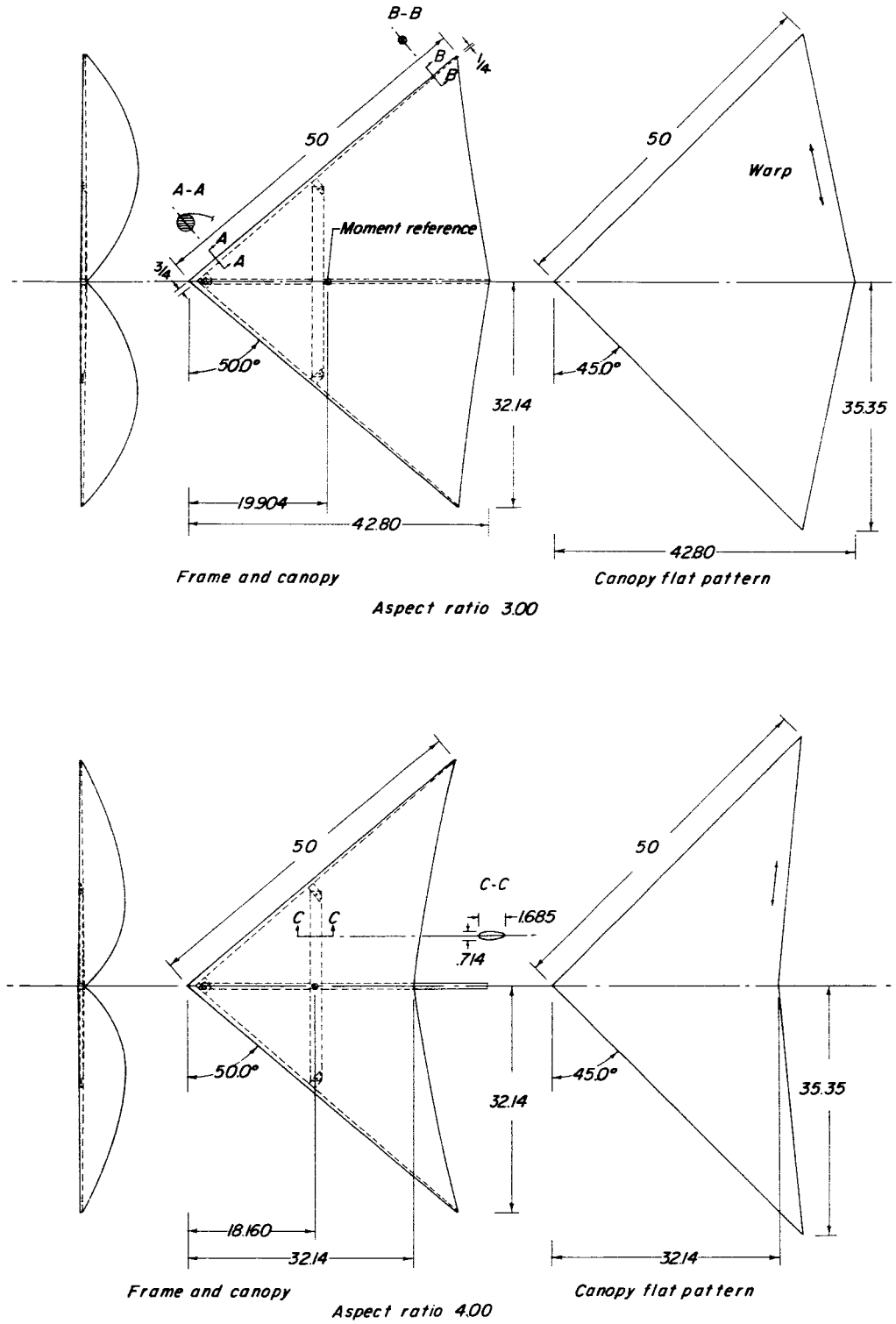

Figure 2.- Geometry of conical parawings. All dimensions are in inches unless otherwise indicated.

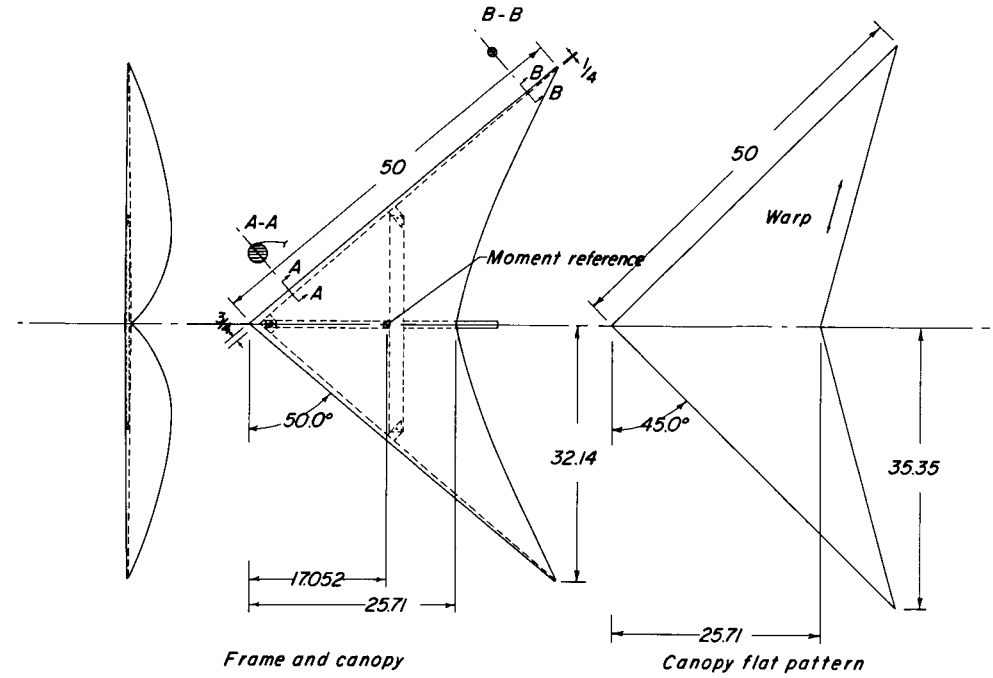

Aspect ratio 5.00

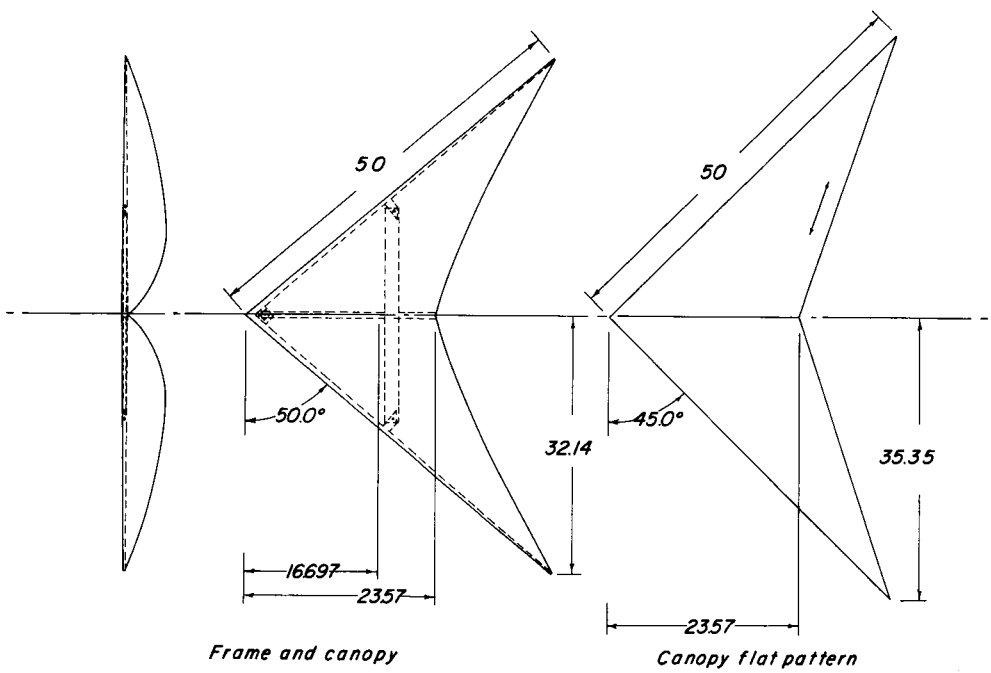

Aspect ratio 5.45

Figure 2.- Concluded.

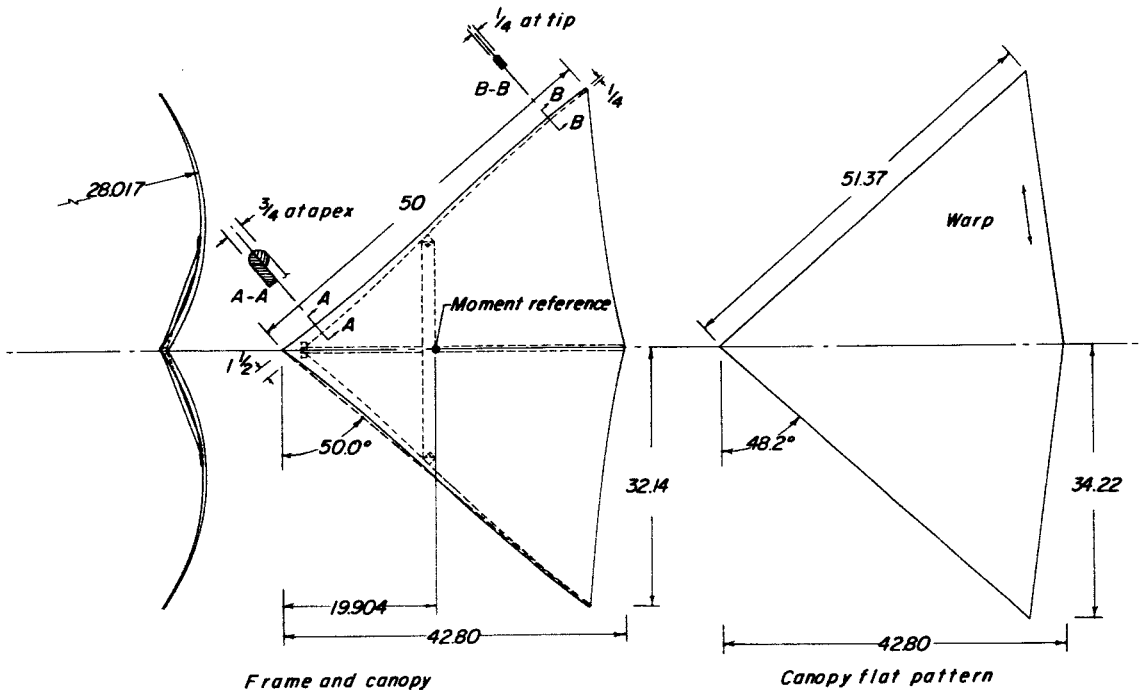

Aspect ratio 3.00

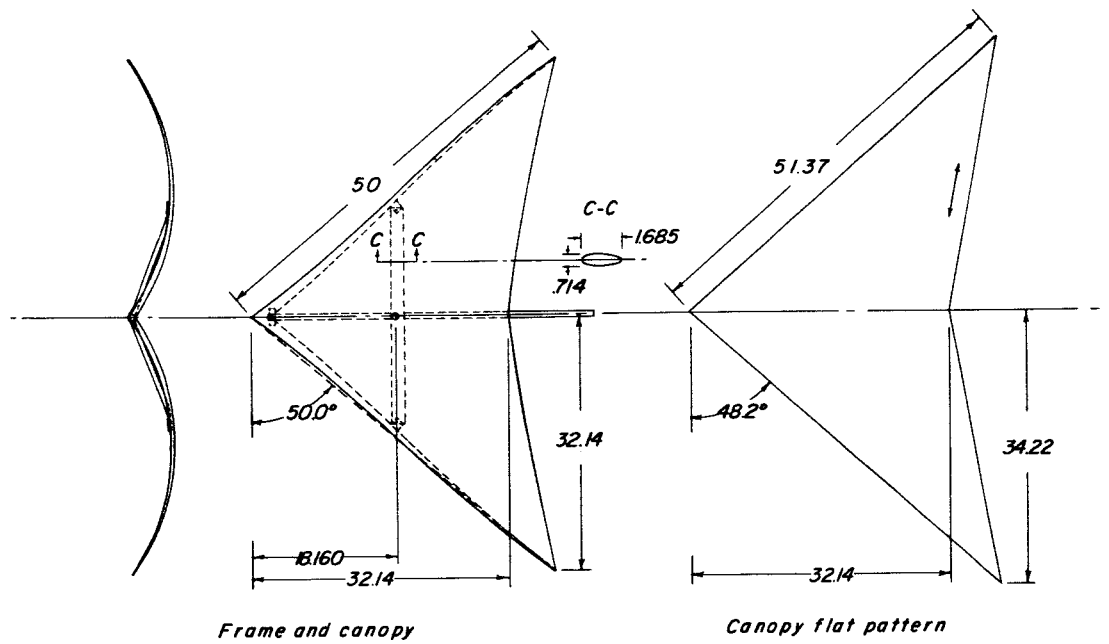

Aspect ratio 4.00

Figure 3.- Geometry of cylindrical parawings. All dimensions are in inches unless otherwise indicated.

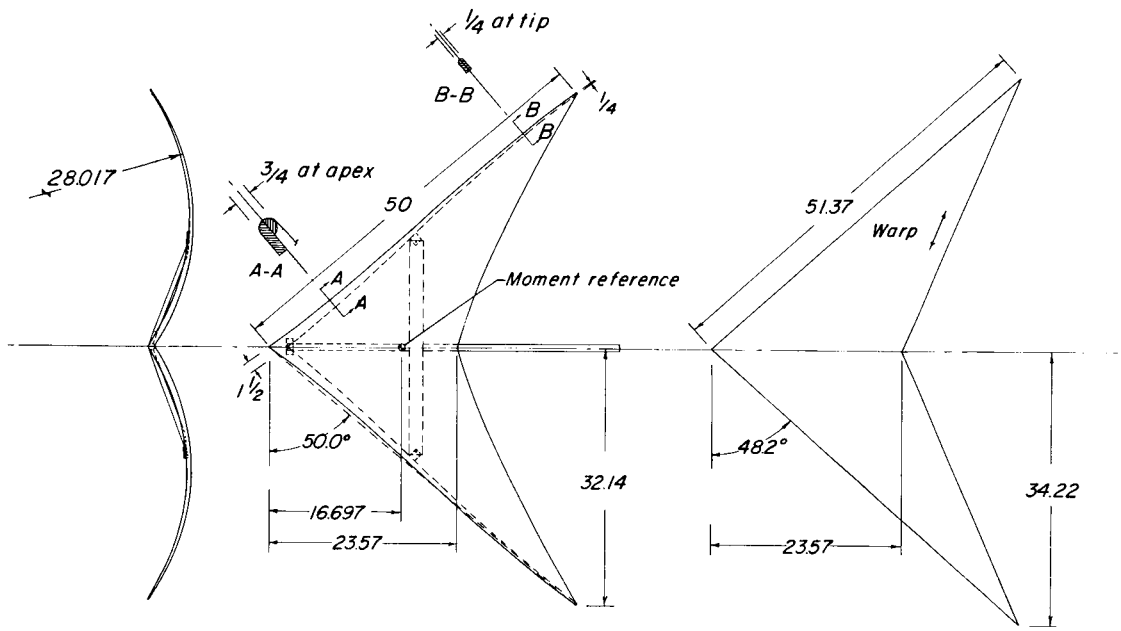

Aspect ratio 5.45

Figure 3.- Concluded.

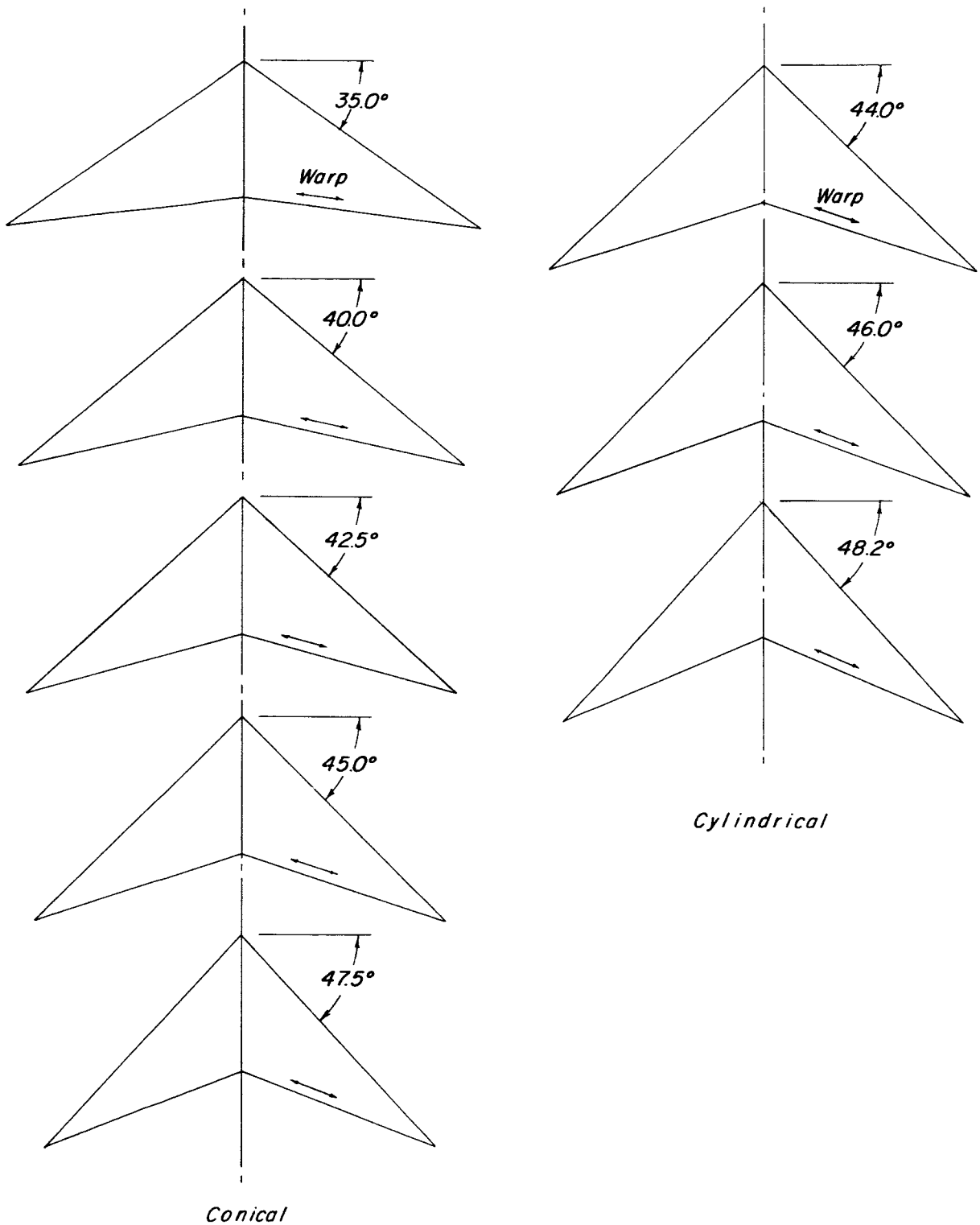

Figure 4.- Canopy flat patterns for the aspect-ratio-5.45 parawings.

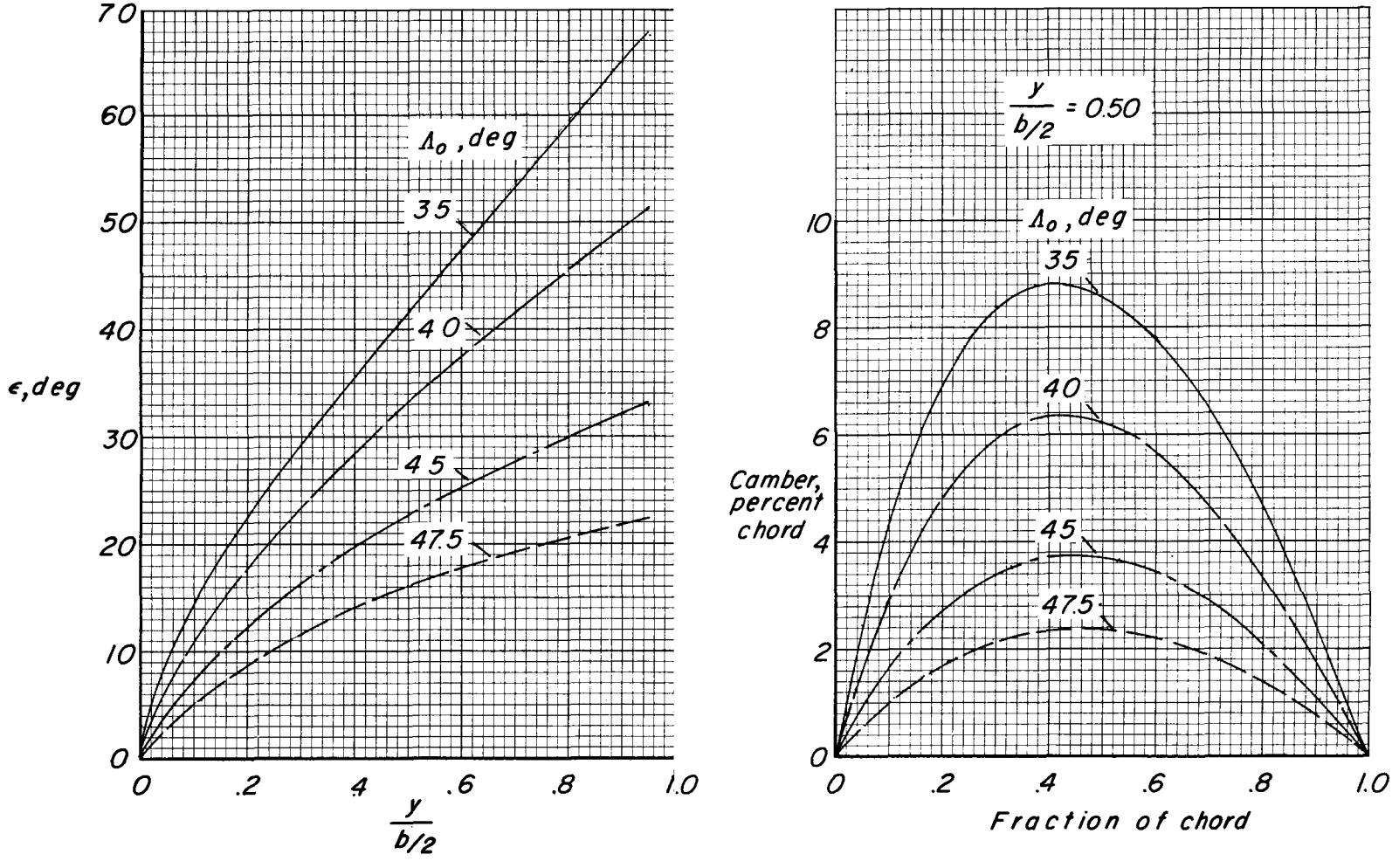

Figure 5.- Twist and camber variation for A = 5.45 conical parawings.

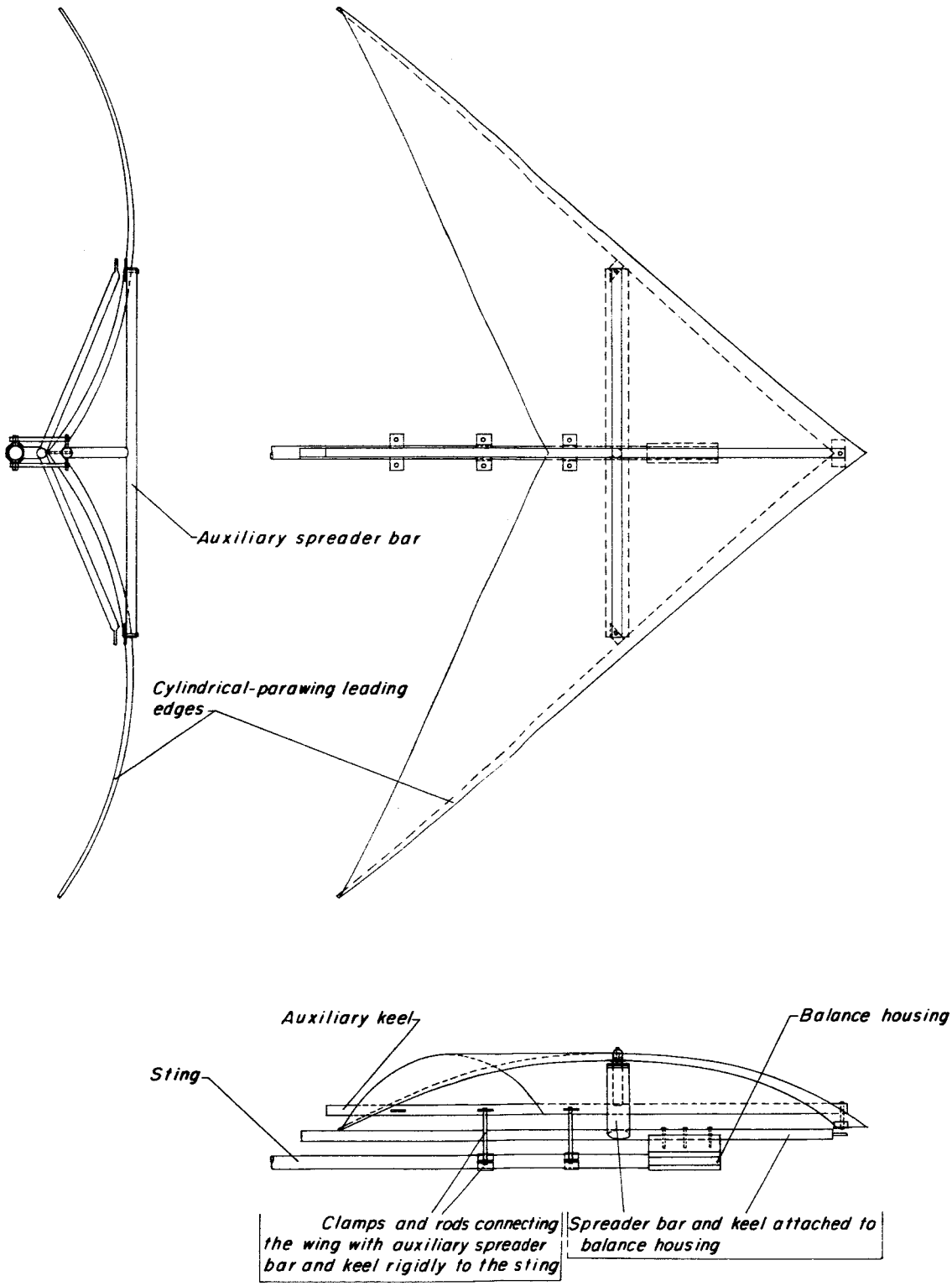

Figure 6.- Spreader-bar and balance-housing tare measurement apparatus.

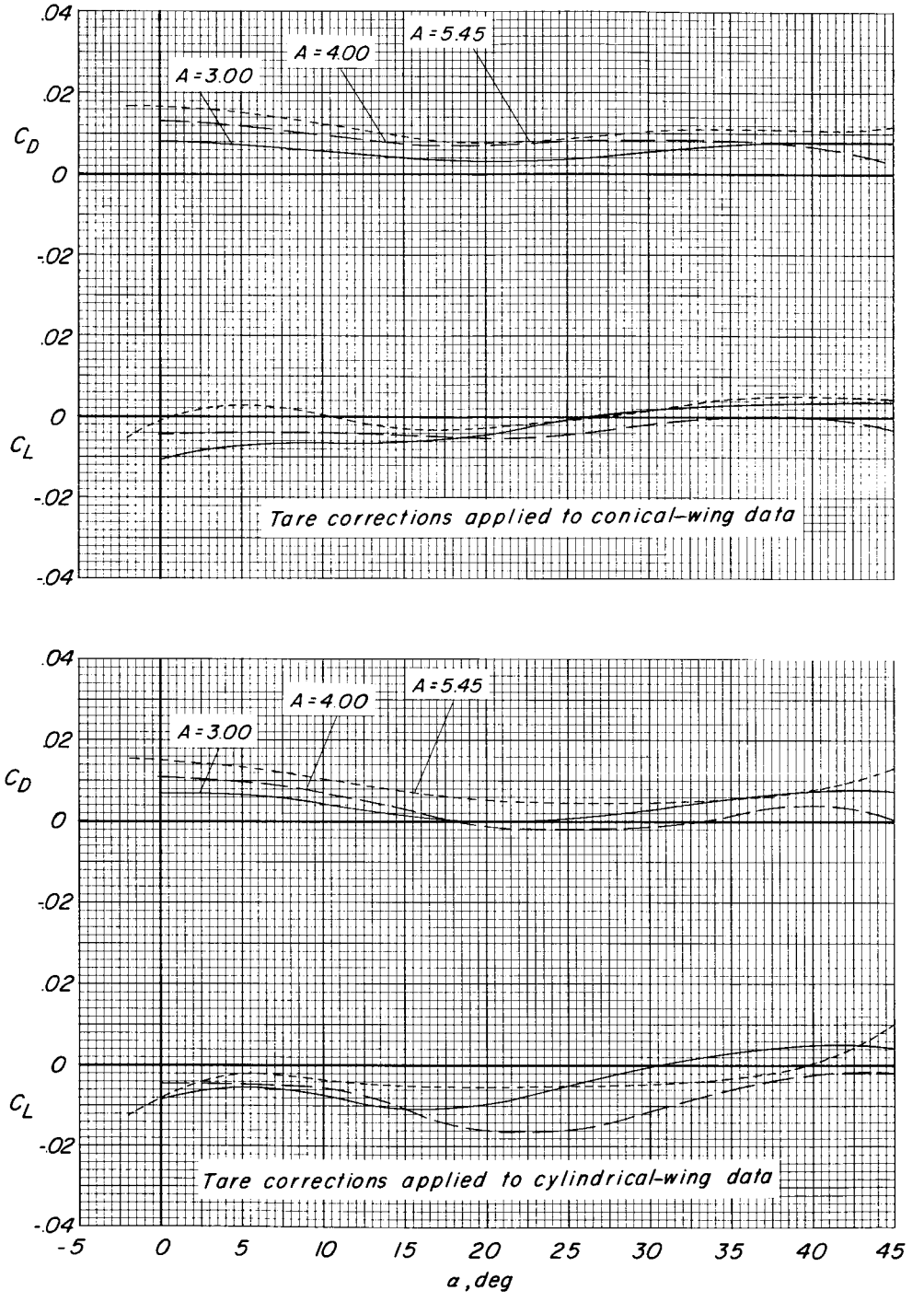

Figure 7.- Aerodynamic characteristics of cylindrical-wing spreader bar and balance housing.

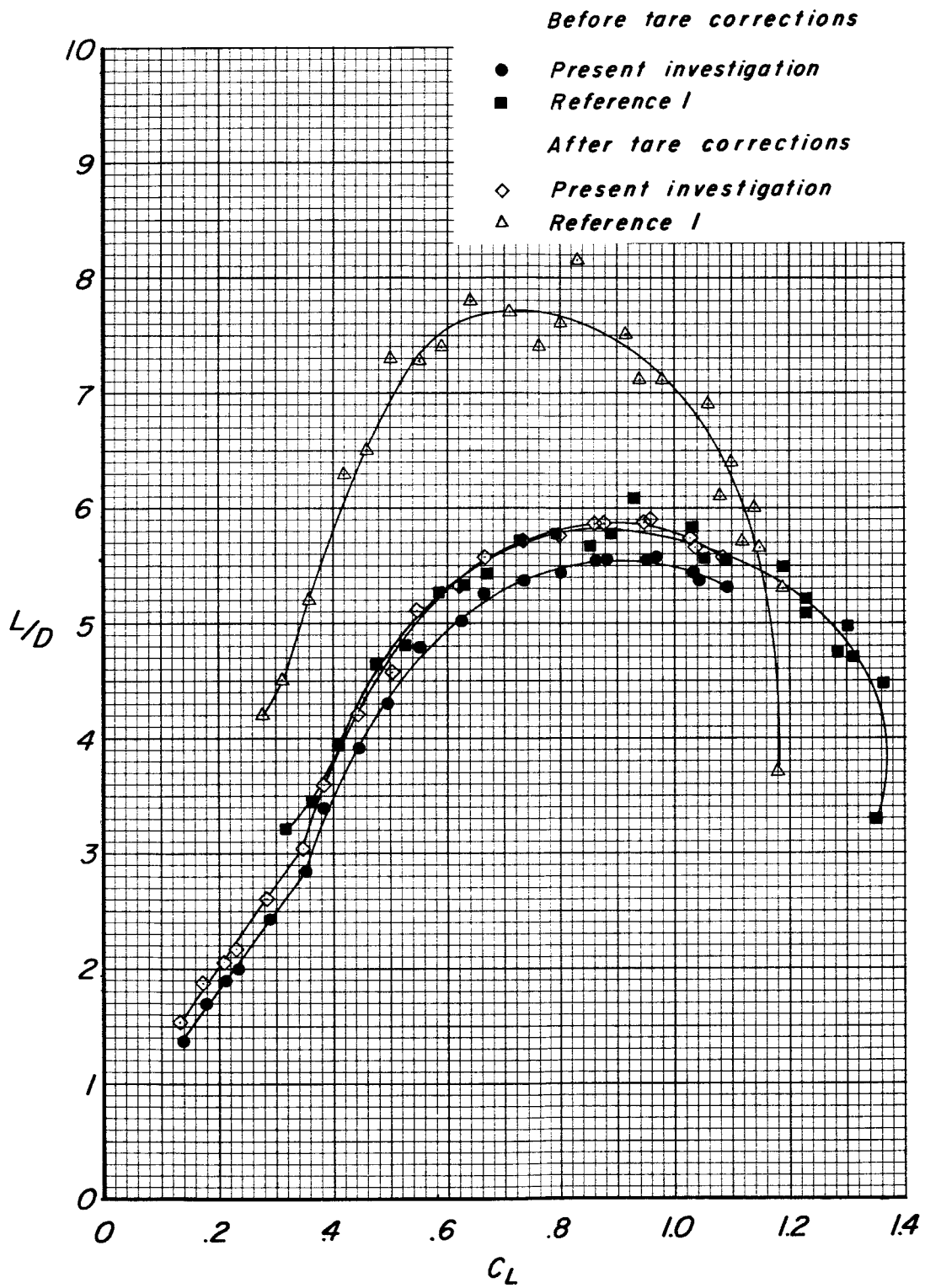

Figure 8.- Conical-wing lift-drag ratios before and after spreader-bar and balance-housing tare corrections for $A = 5.45$, $\Lambda_0 = 45.0^0$.

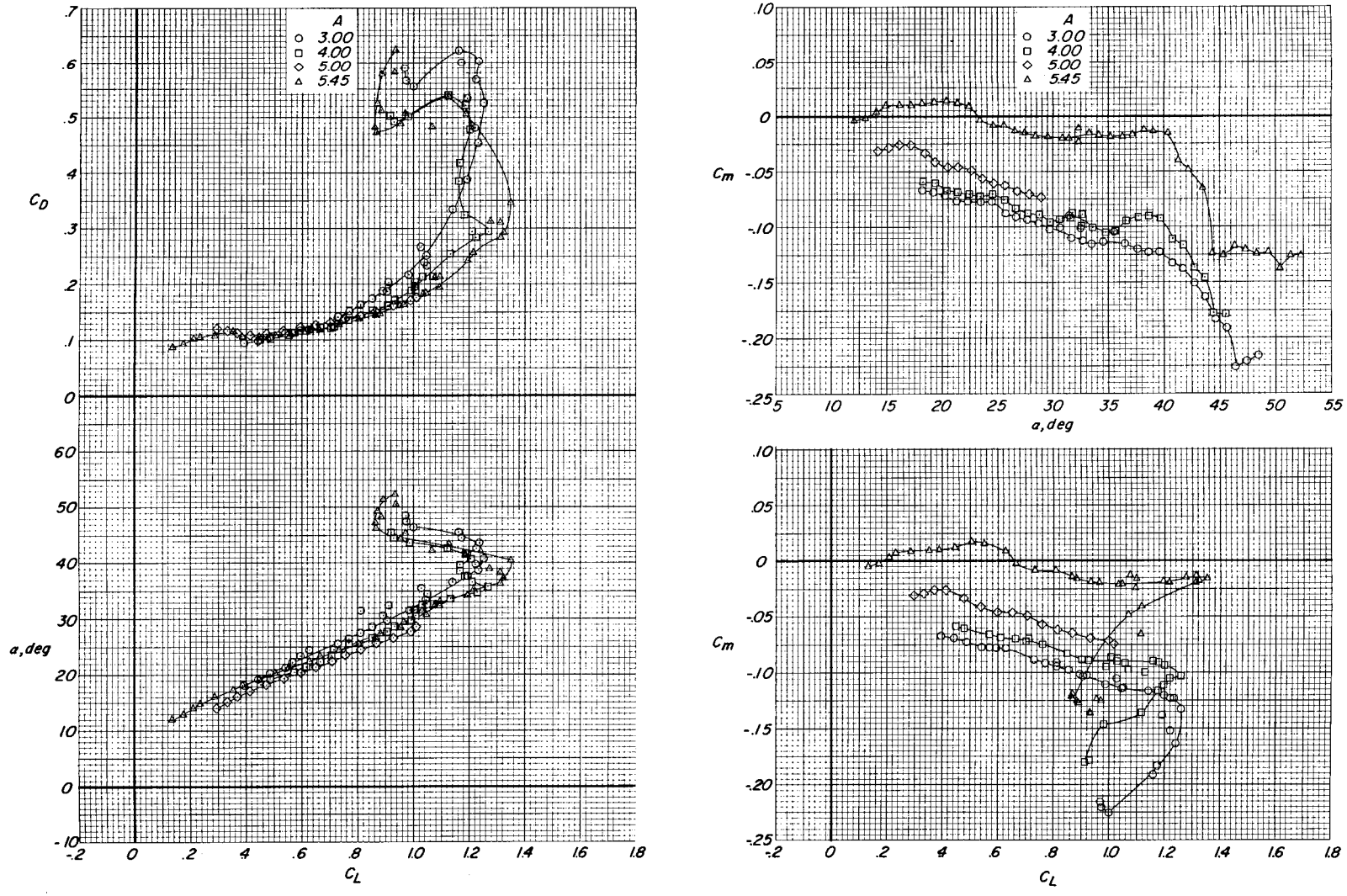

Figure 9.- Effect of aspect ratio on longitudinal aerodynamic characteristics of 50.0° swept conical parawings. $\Lambda_0 = 45.0°$.

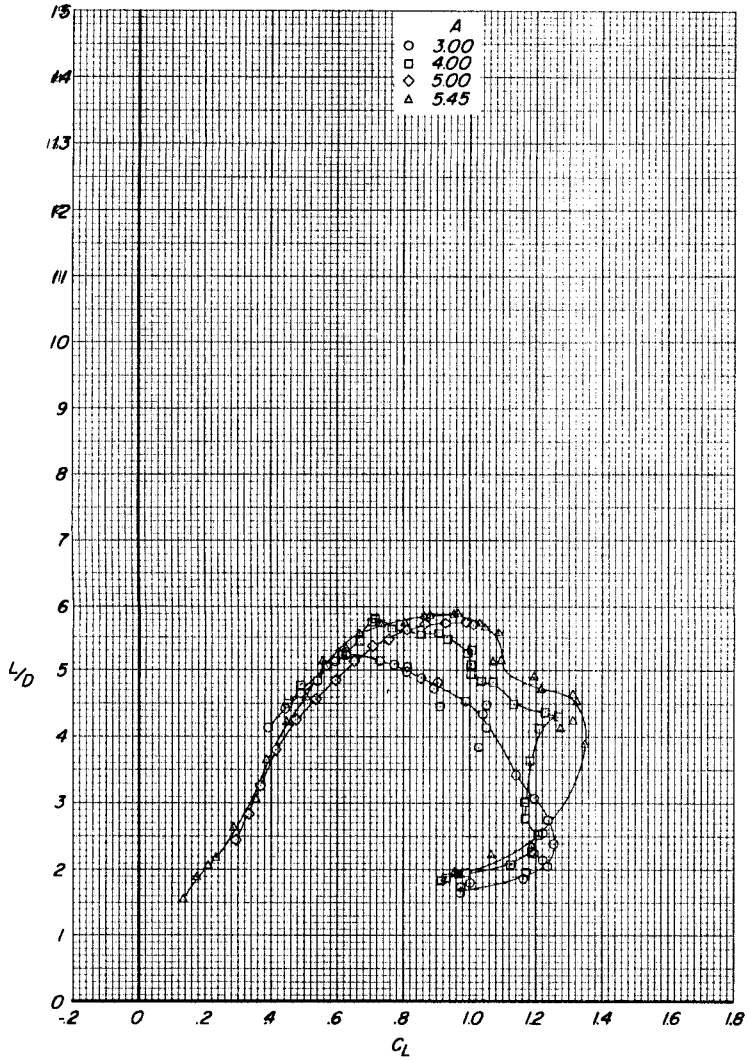

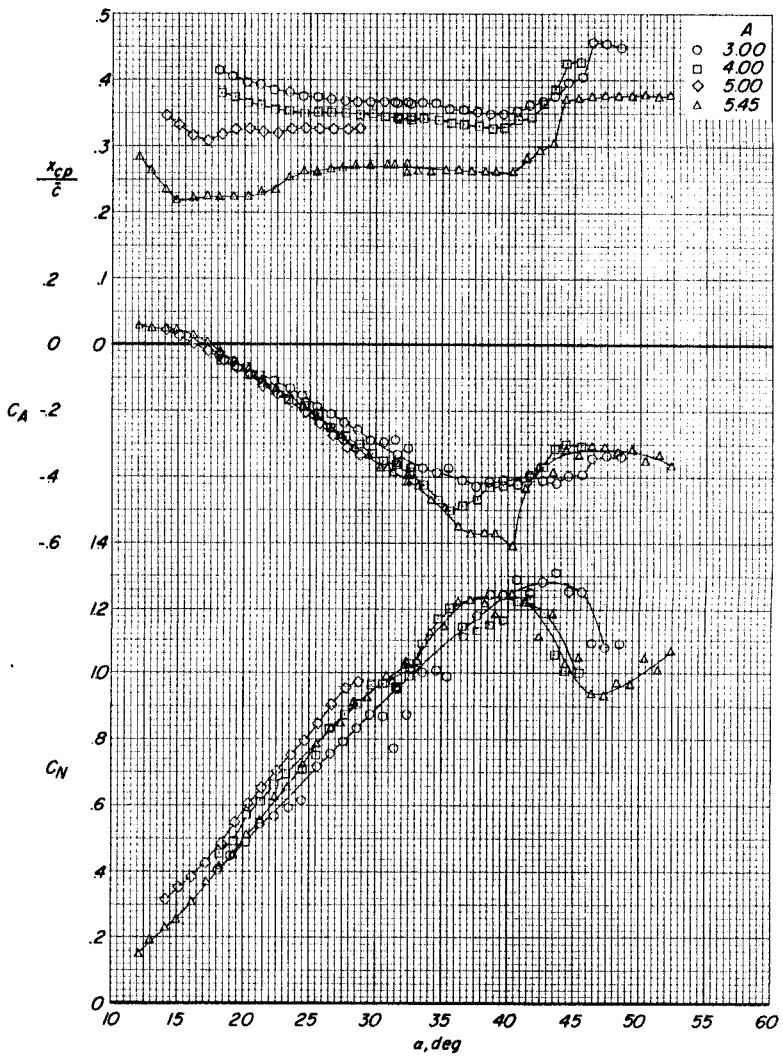

Figure 9.- Concluded.

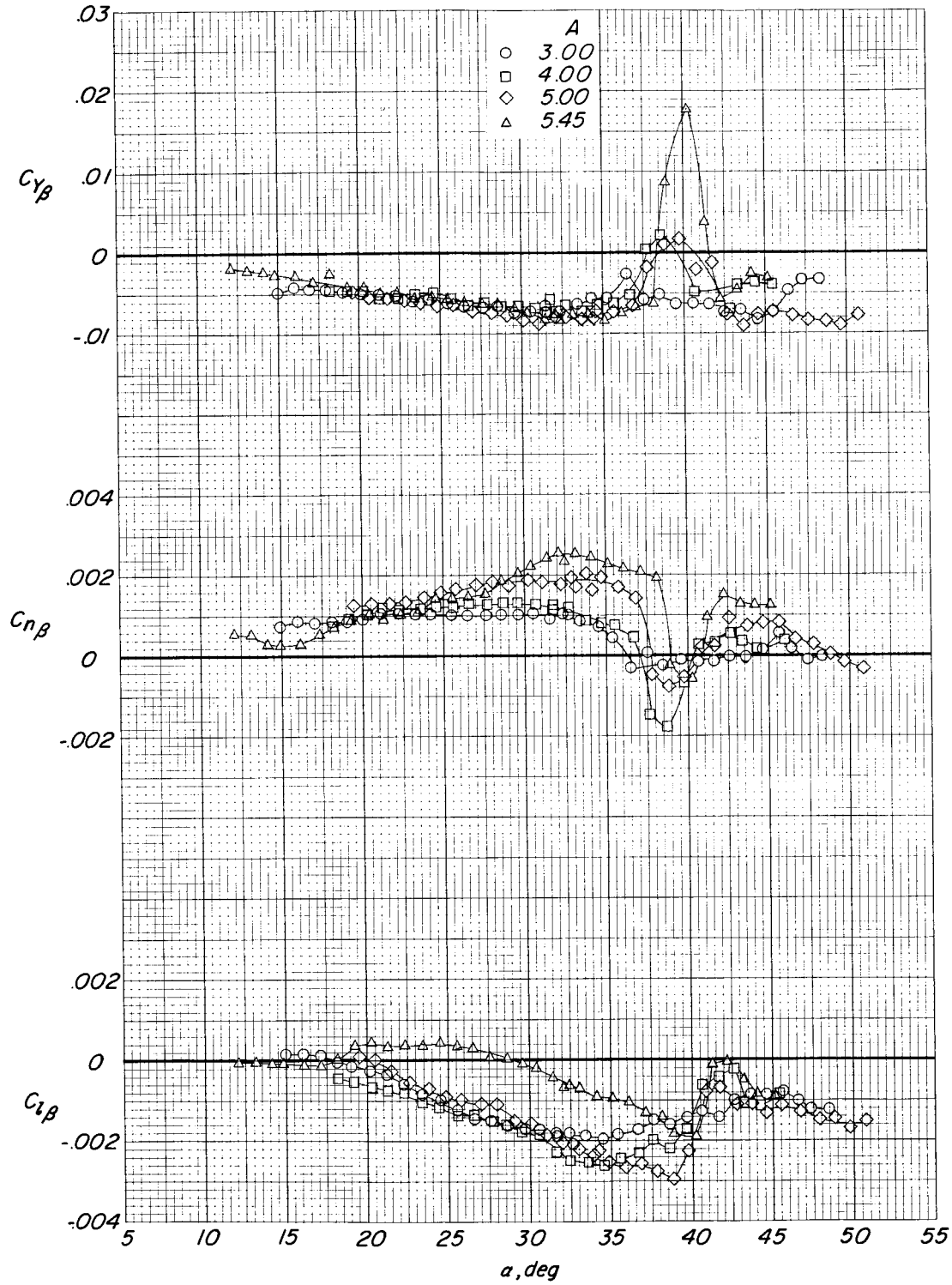

Figure 10.- Effect of aspect ratio on lateral stability characteristics of 50.0° swept conical parawings. $\Lambda_0 = 45.0°$.

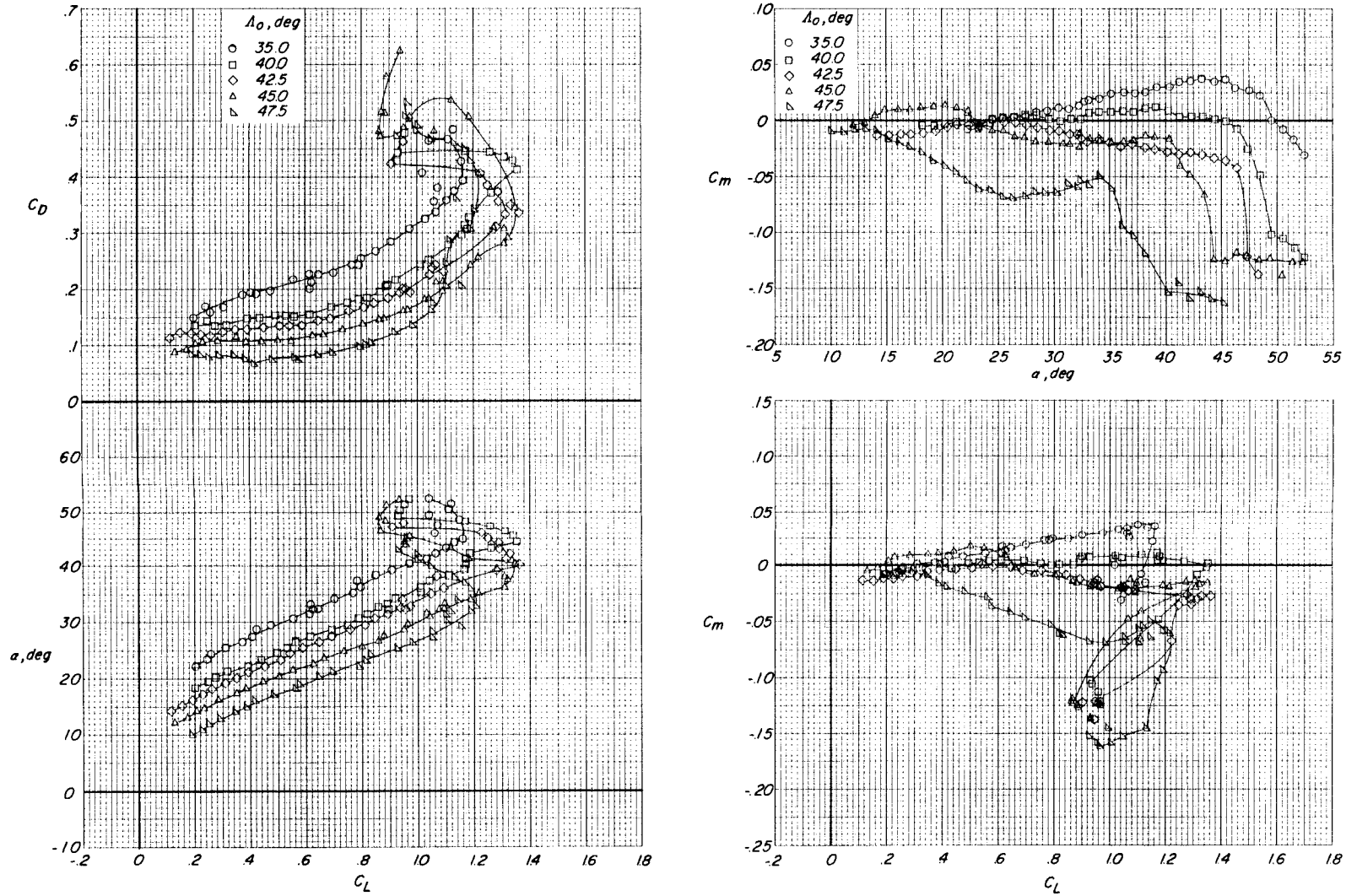

Figure 11.- Effect of canopy-flat-pattern sweep on longitudinal aerodynamic characteristics of 50.0° swept conical parawings. A = 5.45.

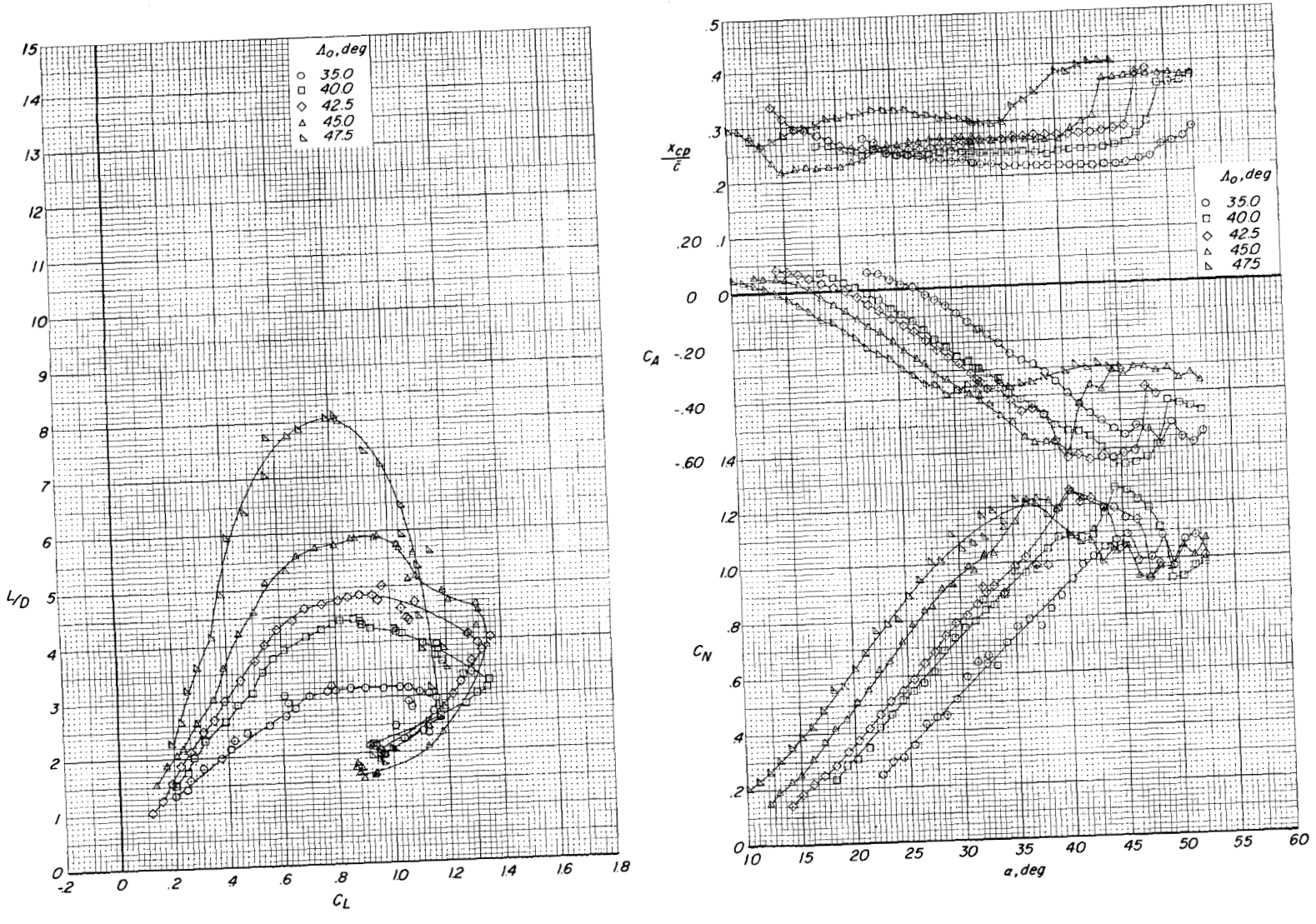

Figure 11.- Concluded.

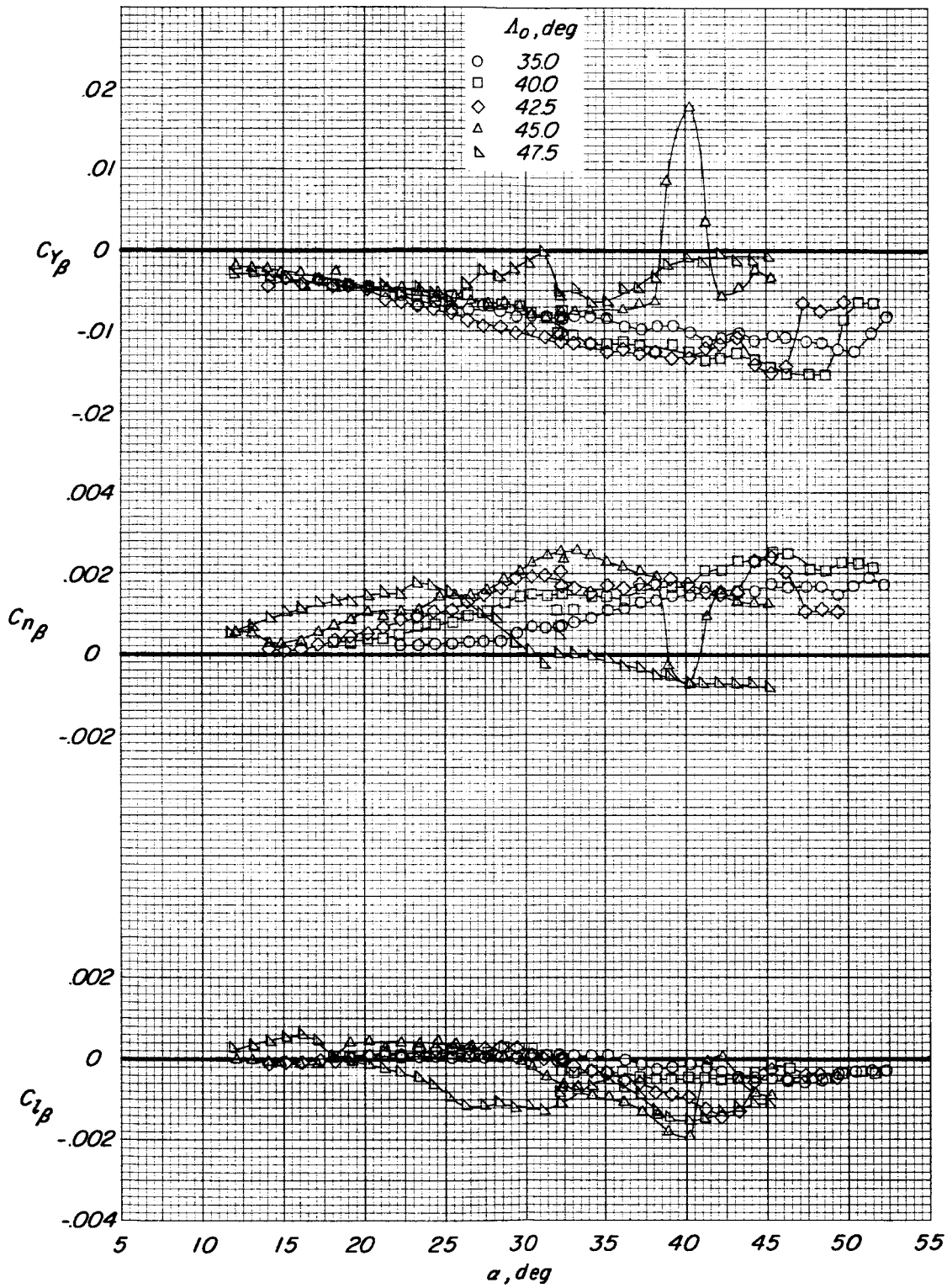

Figure 12.- Effect of canopy-flat-pattern sweep on lateral stability characteristics of 50.0° swept conical parawings. A = 5.45.

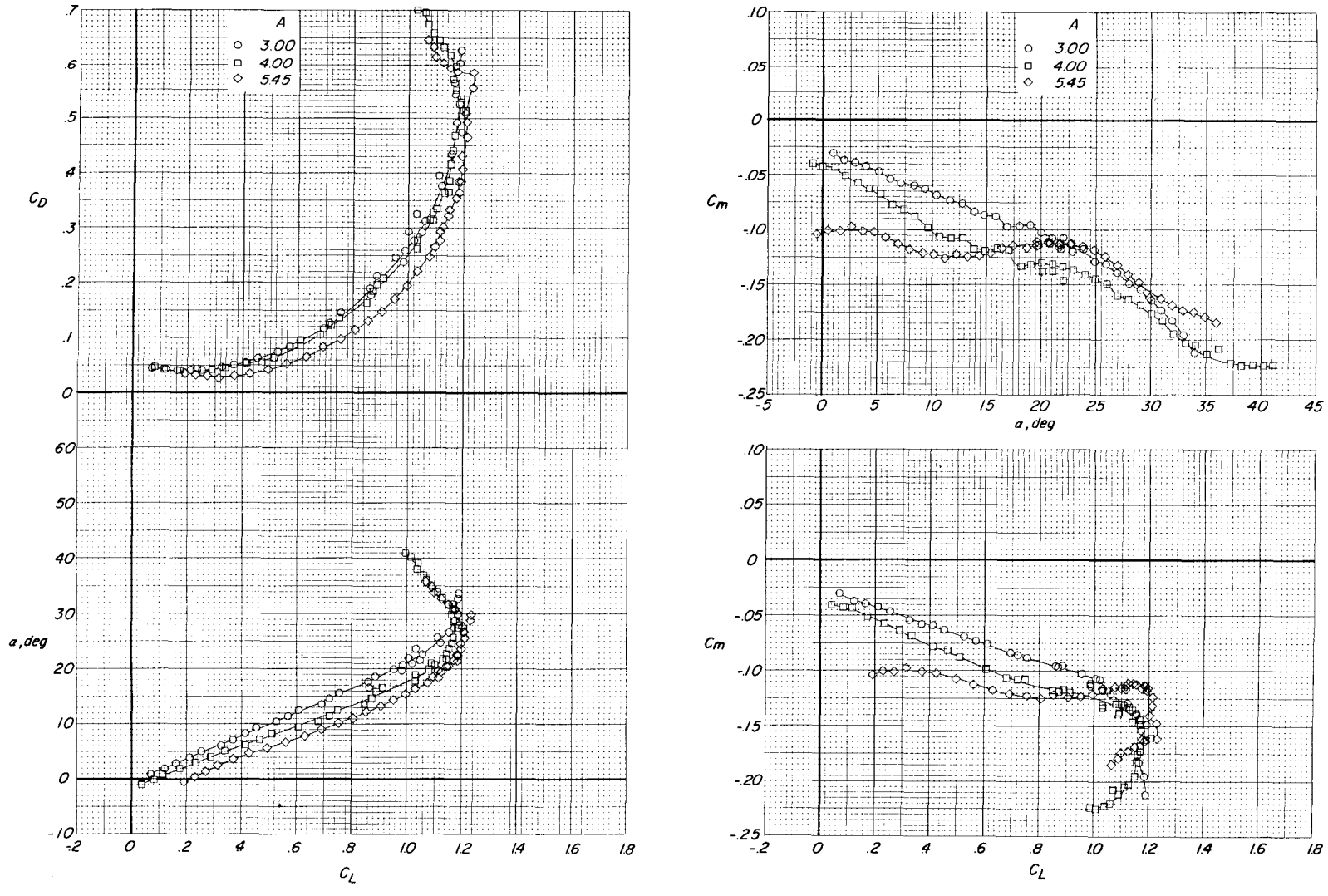

Figure 13.- Effect of aspect ratio on longitudinal aerodynamic characteristics of 50.0° swept cylindrical parawings. $\Lambda_0 = 48.2°$.

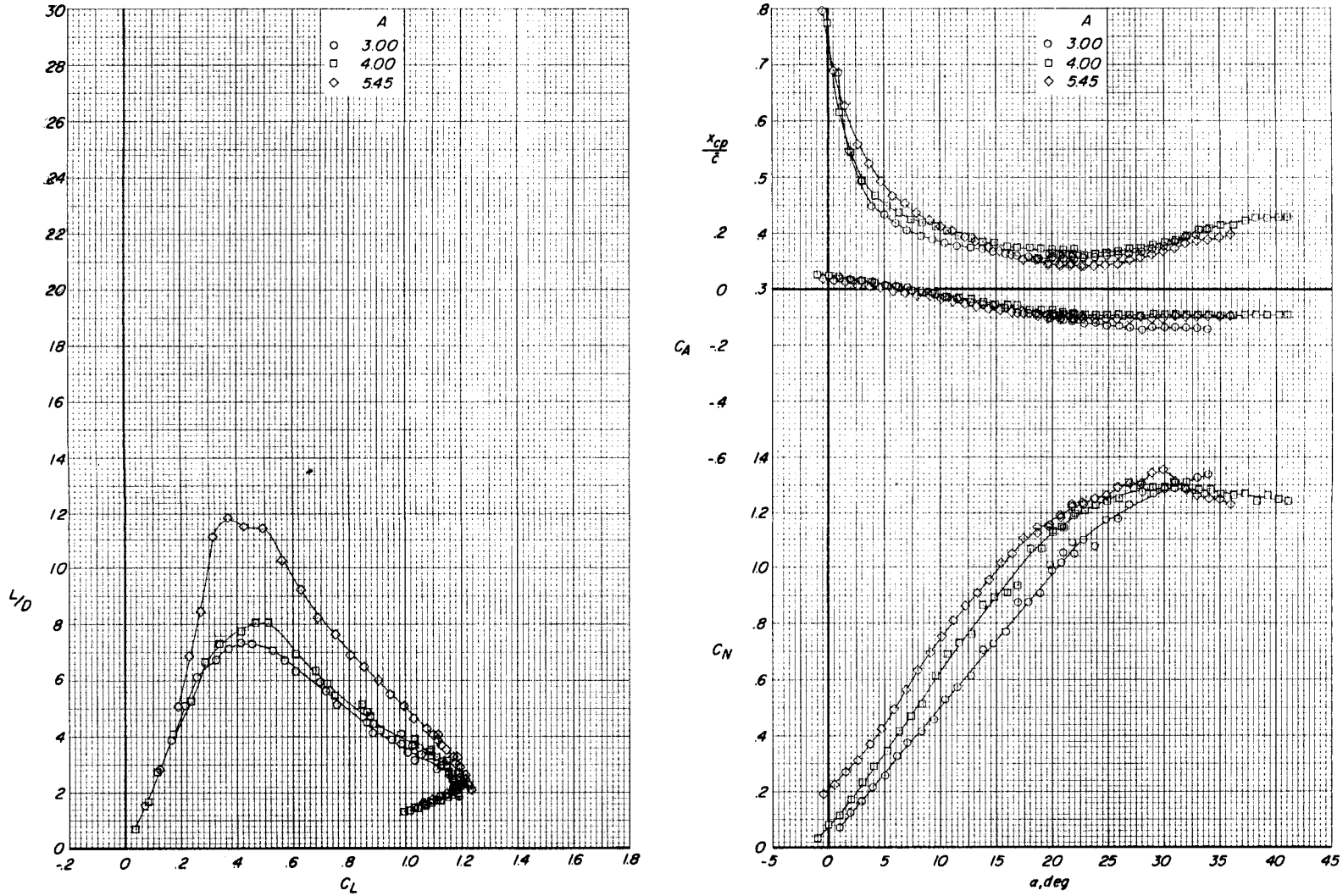

Figure 13.- Concluded.

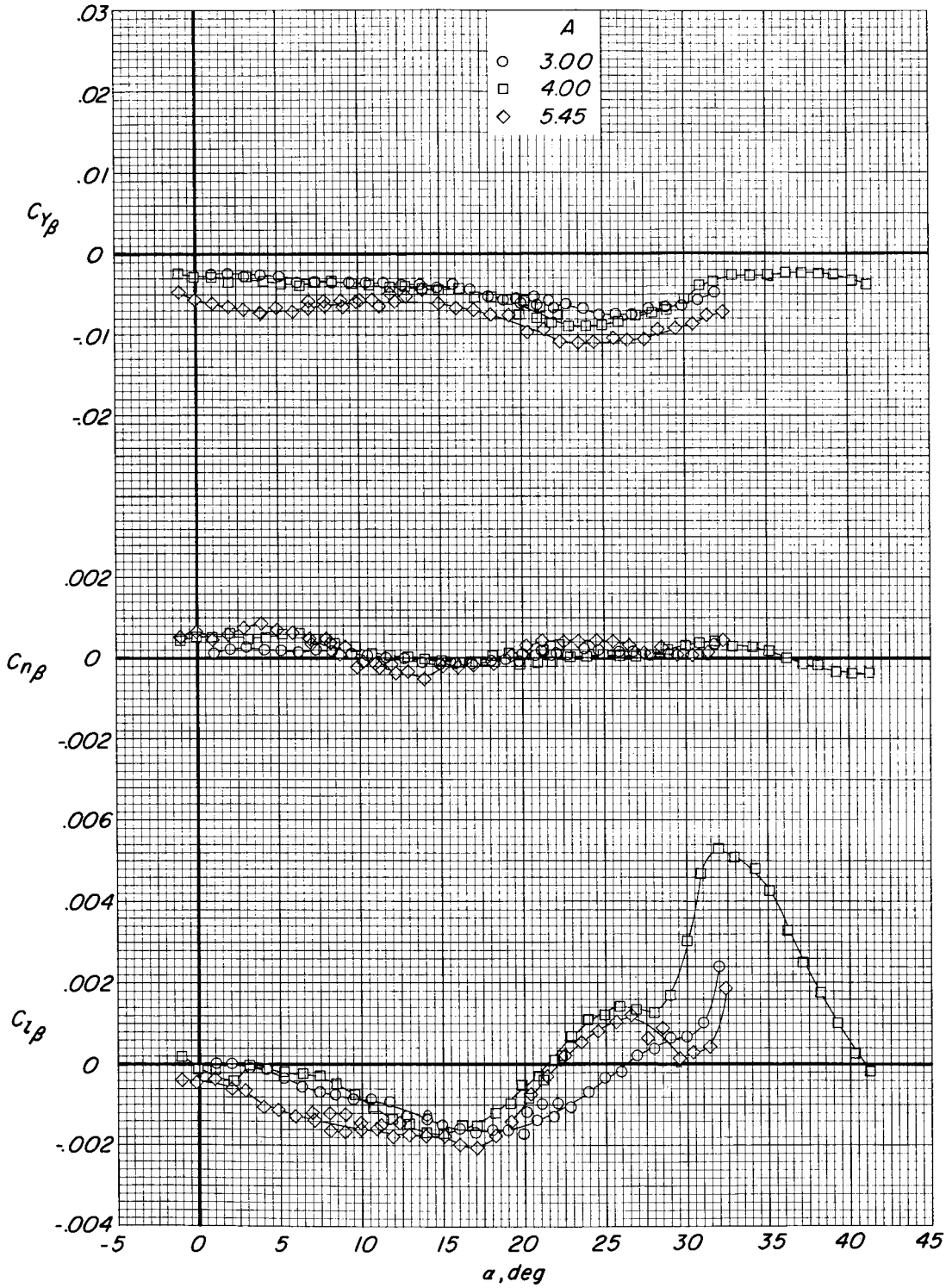

Figure 14.- Effect of aspect ratio on lateral stability characteristics of 50.0° swept cylindrical parawings. $\Lambda_0 = 48.2°$.

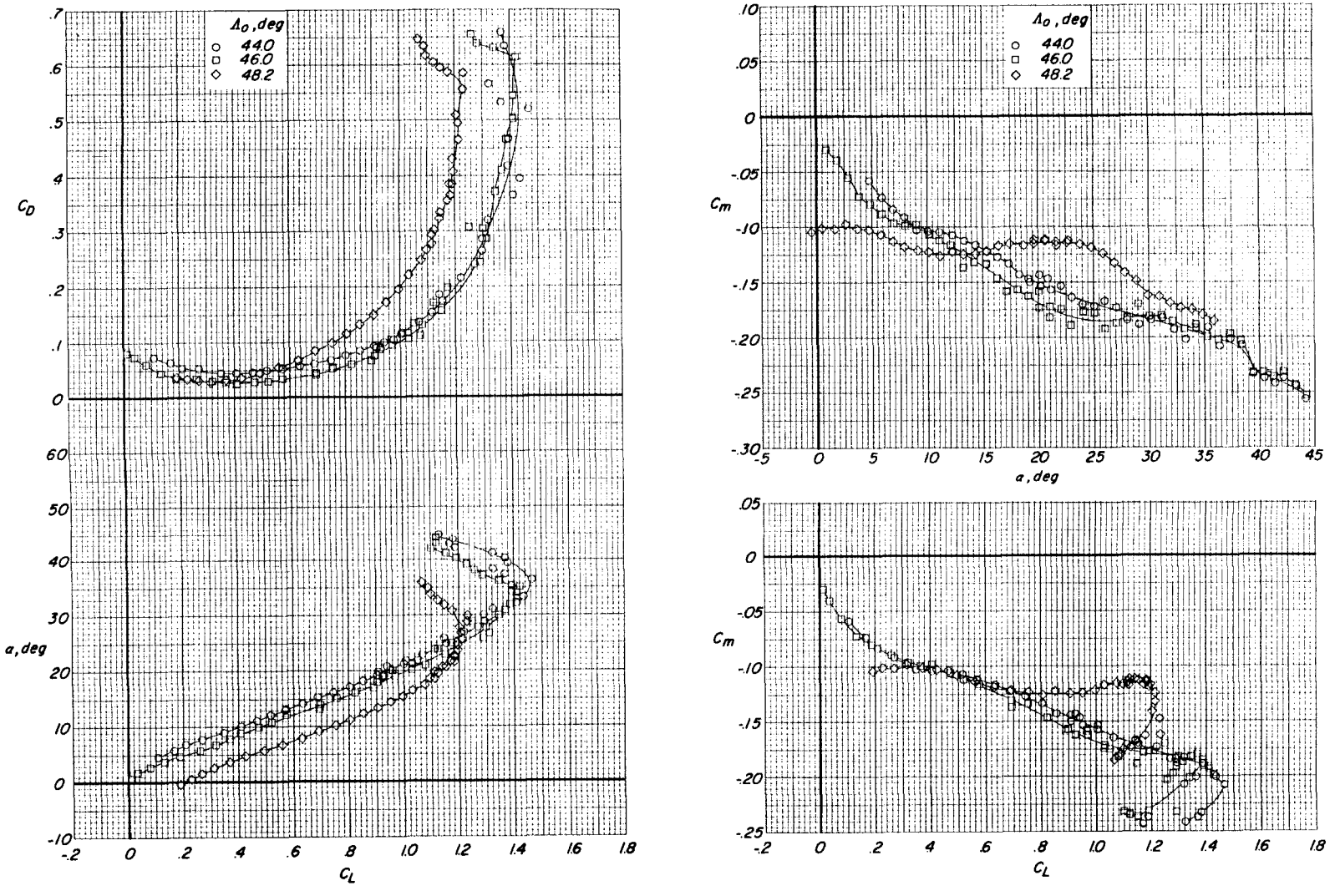

Figure 15.- Effect of canopy-flat-pattern sweep on longitudinal aerodynamic characteristics of 50.0° swept cylindrical parawings. A = 5.45.

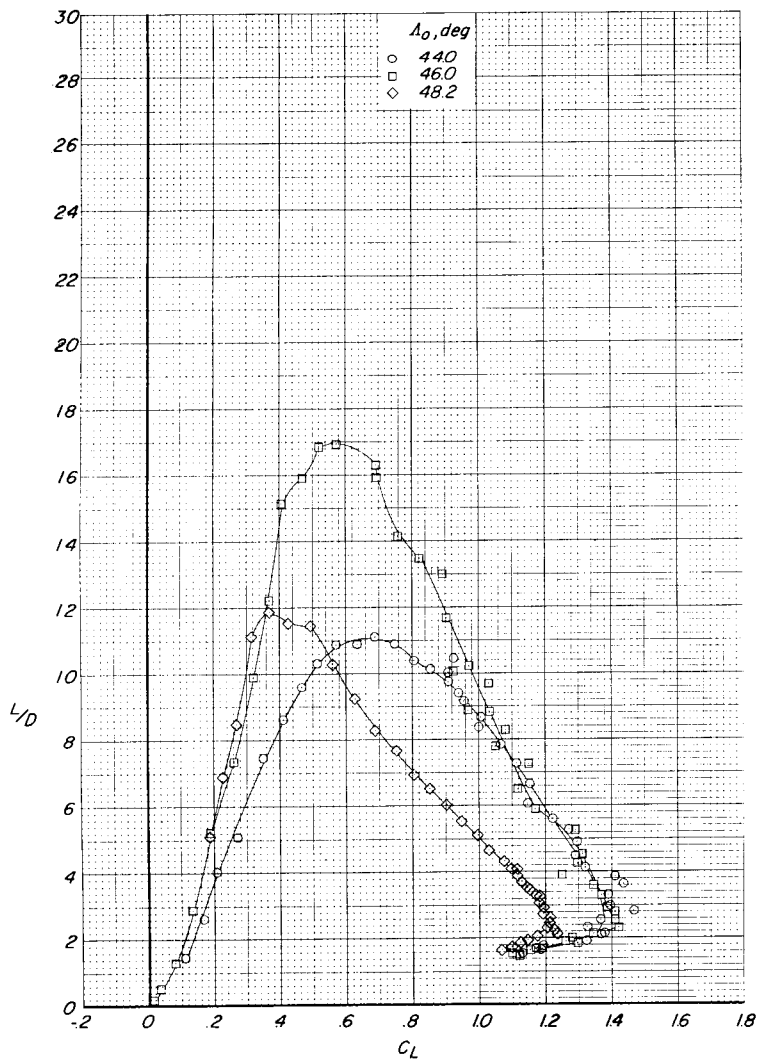

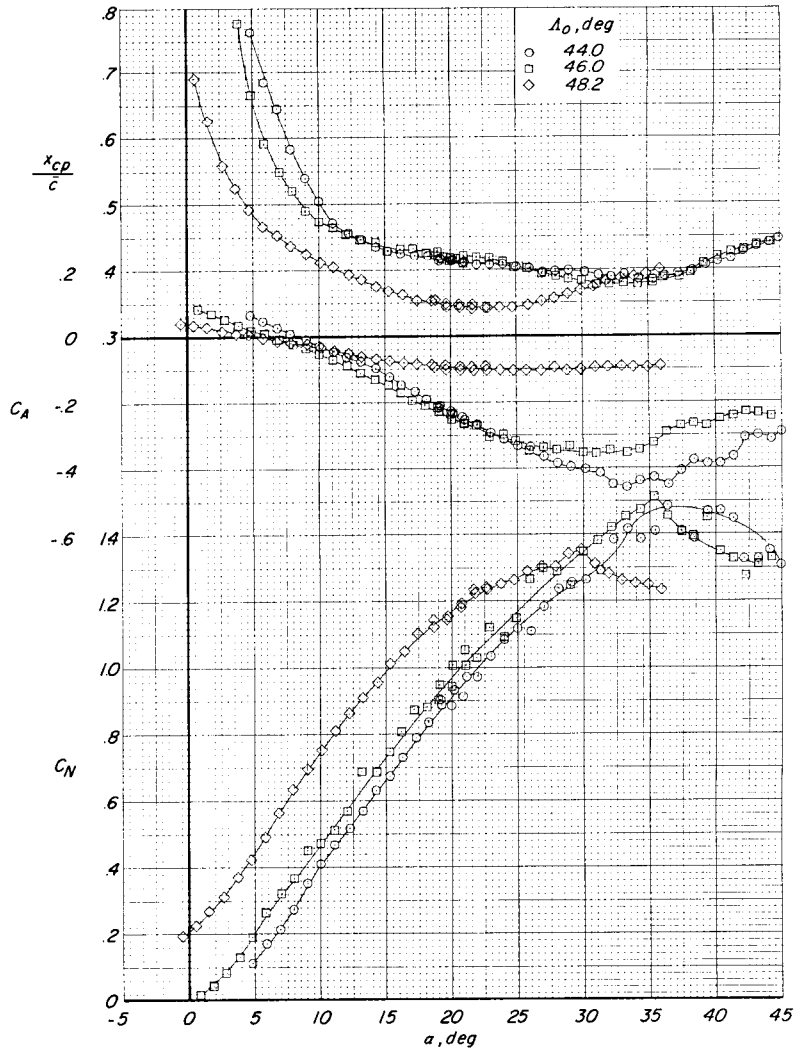

Figure 15.- Concluded.

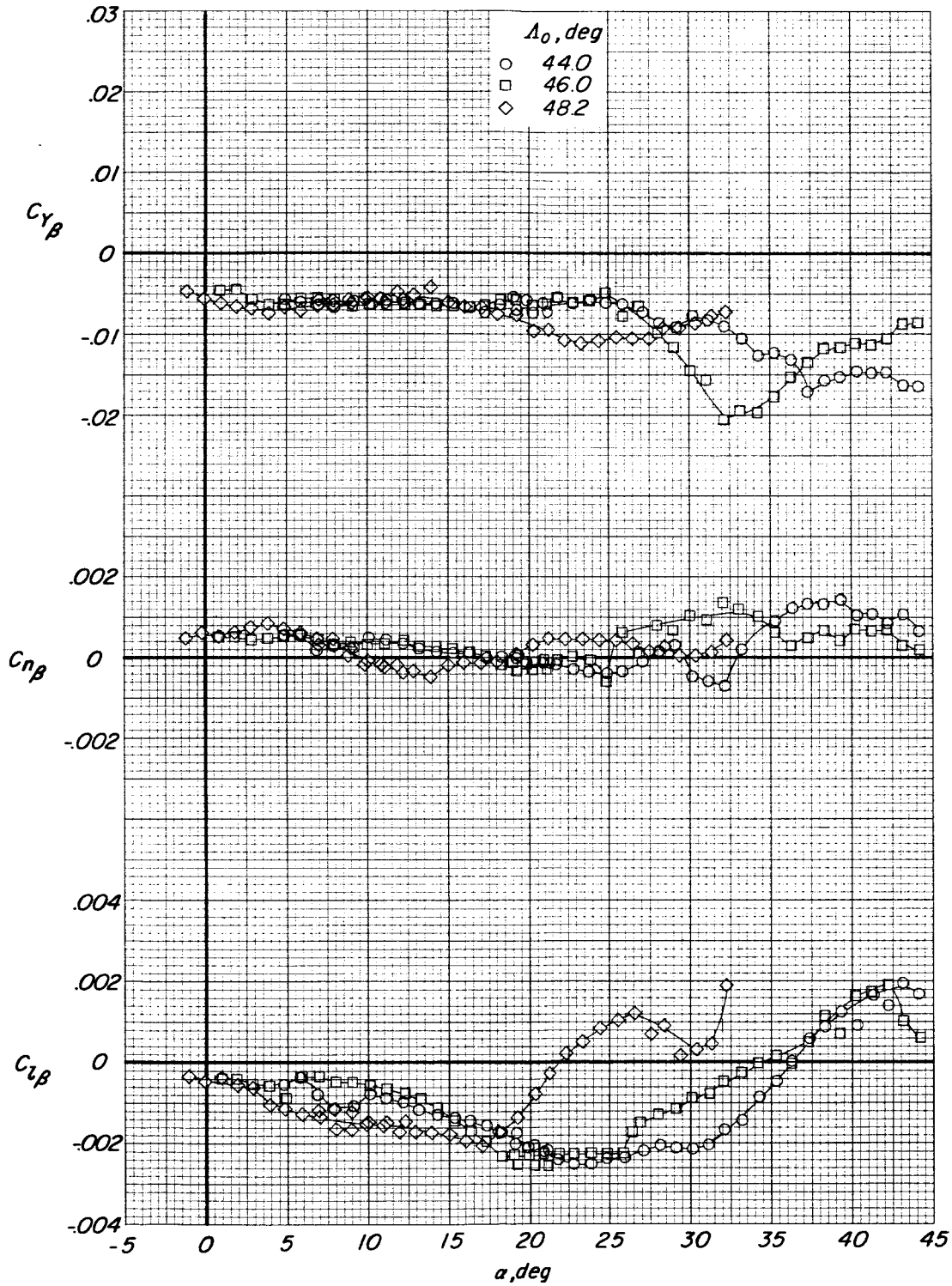

Figure 16.- Effect of canopy-flat-pattern sweep on the lateral stability characteristics of 50.0° swept cylindrical parawings. A = 5.45.

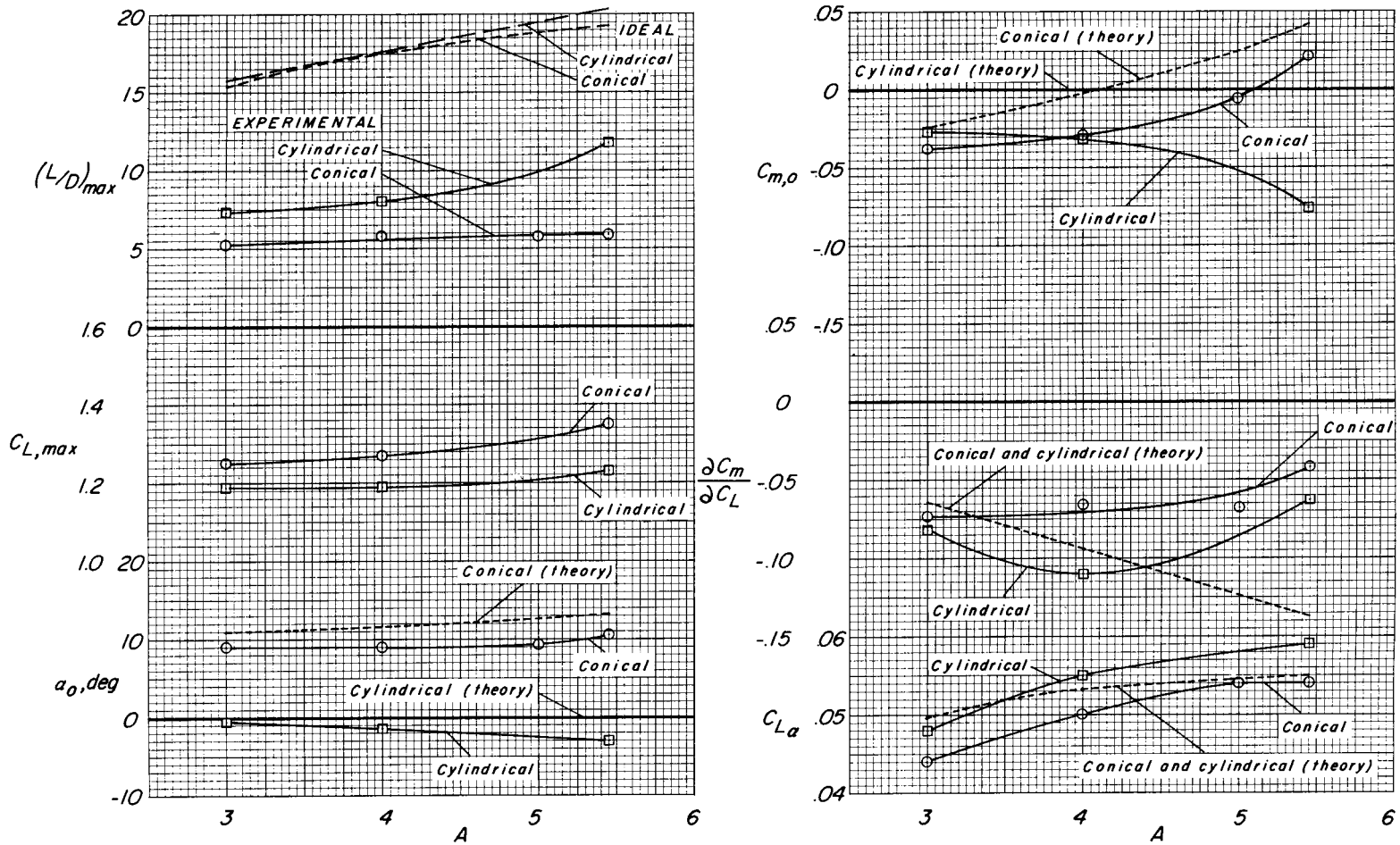

Figure 17.- Summary of effects of aspect ratio on longitudinal aerodynamic characteristics of 50.0^0 swept parawings with conical canopies ($\Lambda_0 = 45.0^0$) and cylindrical canopies ($\Lambda_0 = 48.2^0$).

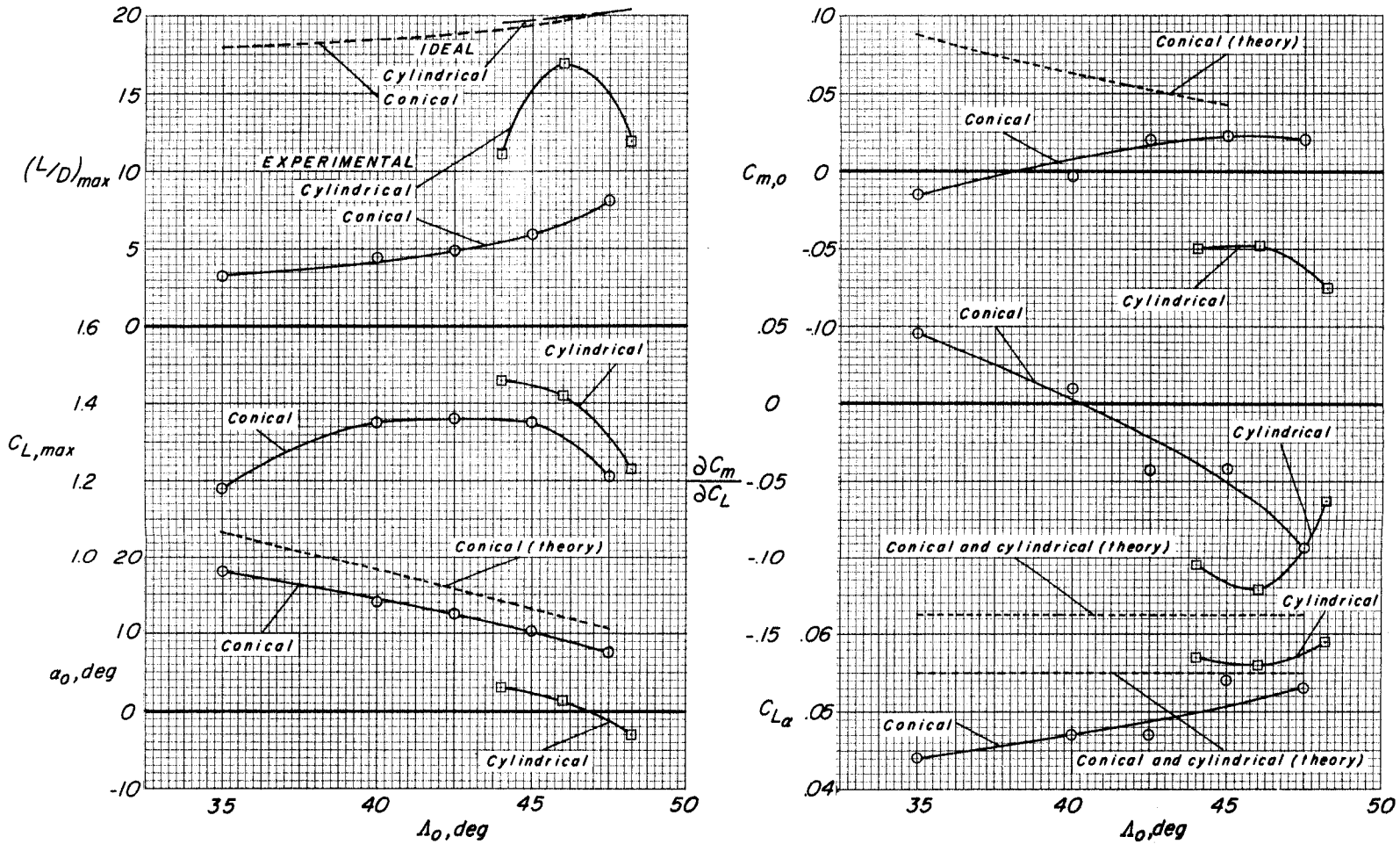

Figure 18.- Summary of effects of canopy-flat-pattern sweep on longitudinal aerodynamic characteristics of 50.0° swept parawings having conical and cylindrical canopies. A = 5.45.

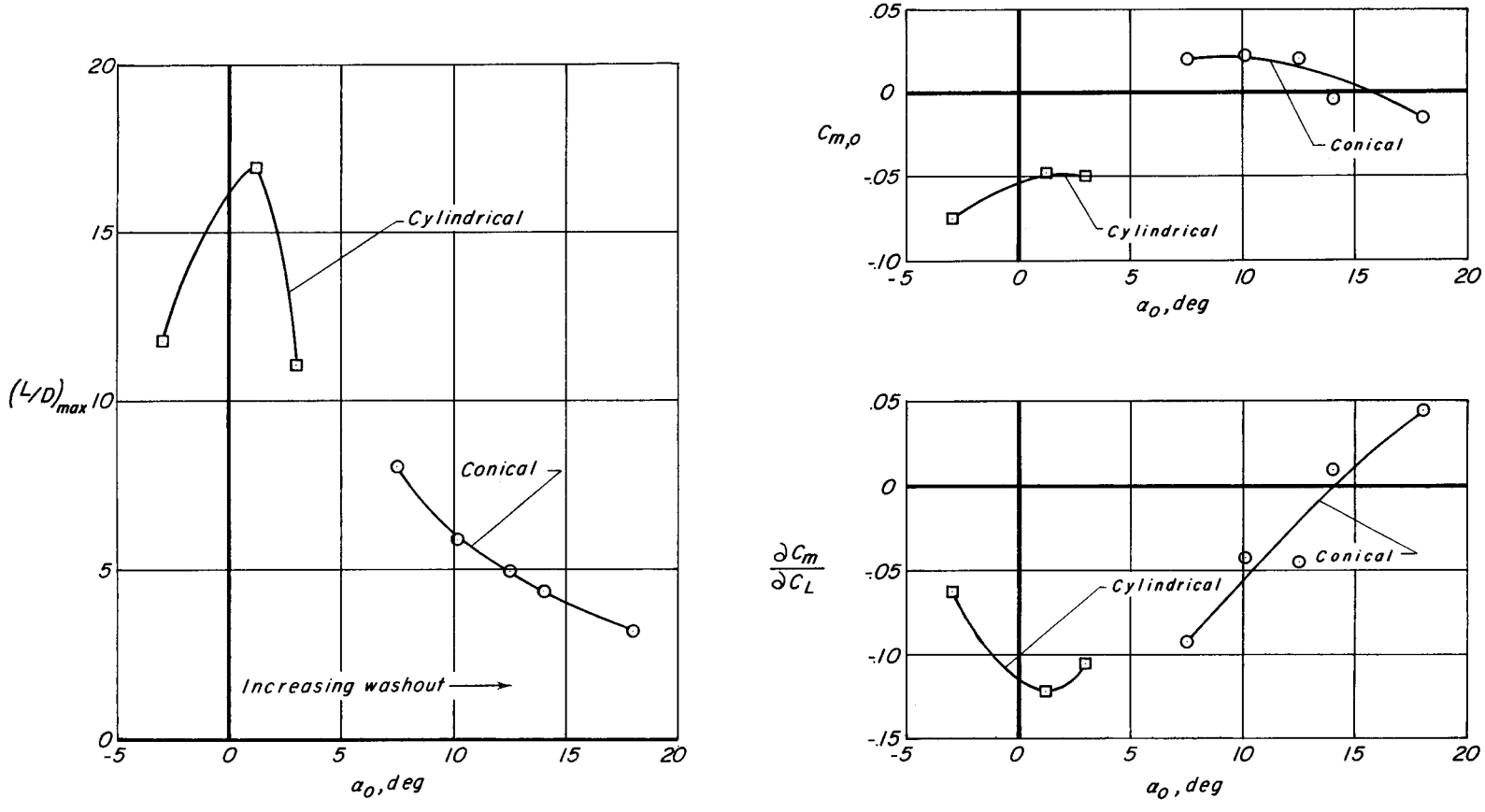

Figure 19.- Summary of effects of zero-lift angle of attack on longitudinal aerodynamic characteristics of 50.0° swept parawings having conical and cylindrical canopies. A = 5.45.